ISSN 1075-7015, Geology of Ore Deposits, 2006, Vol. 48, No. 6, pp. 415–447. © Pleiades Publishing, Inc., 2006.
Original Russian Text © Yu.G. Safonov, V.Yu. Prokof'ev, 2006, published in Geologiya Rudnykh Mestorozhdenii, 2006, Vol. 48, No. 6, pp. 475–511.

Gold-Bearing Reefs of the Witwatersrand Basin: A Model of Synsedimentation Hydrothermal Formation

Yu. G. Safonov and V. Yu. Prokof'ev

Institute of Geology of Ore Deposits, Petrography, Mineralogy, and Geochemistry, Russian Academy of Sciences, Staromonetnyi per. 35, Moscow, 119017 Russia

Received June 22, 2006

Abstract—The current concepts concerning the genesis of the unique ore-bearing reefs of the Witwatersrand Basin and its gold resource potential are considered. The results of microscopic examination of ore from the Black, Ventersdorp Contact, Carbon Leader, and Vaal reefs, as well as of thermobarometric study of quartz, are presented. A model of synsedimentation hydrothermal origin of the reefs in the process of evolution of primary colloidal–disperse systems is substantiated on the basis of these results and the data published by other authors. The formation of these systems is related to the periodic gain of deep ore-bearing gas-saturated fluids. The gold mineralization was formed under conditions of partially closed systems, where various mineral-forming processes developed (metasomatism, crystallization of true solutions and gels, gel metasomatism, dispersion of crystalline phases, segregation of mineral particles, formation of early minerals, etc.). New data on REE specialization of ore-bearing fluids are discussed. The specific features of the gold, carbonic, and uranium mineralization of the intracratonic basin are emphasized.

DOI: 10.1134/S1075701506060018

INTRODUCTION

The relentless interest in the genesis of the unique gold concentrations in the Witwatersrand Basin is fueled not only by the scope of these concentrations but also by their implications for the metallogeny of gold in general, the theory of gold deposit formation, and the geology of ore deposits as a whole.

The most popular concept of gold-bearing reefs of the Witwatersrand Basin as altered and metamorphosed primary placers (Viljoen et al., 1970) inevitably poses the question of the source of these placers, which should be still more extraordinary gold deposits and provinces formed more than 3 Ga ago. Such deposits and provinces are unknown to date.

Another aspect of the problem is related to the metallogeny of intracratonic basins, which are characterized by polygenetic ore mineralization. This aspect is becoming increasingly important for Russian geology. The ideas of polygenetic and staged ore mineralization developing at the Institute of Geology of Ore Deposits, Petrography, Mineralogy, and Geochemistry, Russian Academy of Sciences, mainly with respect to uranium deposits (Laverov et al., 1986), gained renewed impetus from the study of untraditional gold deposits, as may be exemplified by the Sukhoi Log deposit with complex PGE–Au mineralization (Laverov et al., 1997). The effect of tectonic and metallogenic prehistory (the history of the Riphean intracontinental basin in the above example) on the subsequent formation of ore deposits has been pointed out for various provinces (Rundquist, 1993, 1997; Safonov, 1997).

The aforementioned problems and the unique character of the deposits in the Witwatersrand Basin attract keen interest. An immediate acquaintance with the deposits of the Witwatersrand Basin, the examination of collected samples, and a survey of the voluminous literature allows us to state own opinion concerning the origin of the Witwatersrand ore-bearing reefs and to provide new insights into the conditions and mechanisms of ore formation.

The microscopic examination of ore was focused on revealing typomorphic features of quartz and pyrite as major minerals of the reefs that bear information on ore genesis. The same objective was set for the thermobarometric study of quartz. Additional information was extracted from numerous publications; however, this was not a simple task because of the abundant factual data and their frequent interpretation in terms of specific genetic concepts. The original data were obtained from the examination of samples collected by Yu.G. Safonov during his visit in 1998 to the mines of the Anglogold Company in the western goldfields Carletonville (West Wits Line) and Klerksdorp and by a survey of the open pits in the East Rand in 2002. The Black Reef is mined in these open pits. In the western goldfields, samples of ores and rocks were taken from underground mines developing the Ventersdorp Contact, Carbon Leader (Carletonville), and Vaal (Klerksdorp) reefs. Local geologists kindly donated samples from the Doornfontein and Kloof mines (Ventersdorp Contact Reef (VCR)) and Welcom goldfield (Basal Reef).

Corresponding author: Yu.G. Safonov. E-mail: safonov@igem.ru

At the first stage of the study, the main attention was paid to the gold mineralization of reefs and the basin as a whole. The study of uranium mineralization has not been completed as yet. This mineralization, which is closely related to kerogen and bitumen, requires a special consideration. This paper is focused on the formation conditions of the main gold mineralization. The concept of ore formation related to synsedimentation hydrothermal activity pertains largely to the gold–pyrite and gold–sulfide–quartz mineral assemblages. Special attention was paid to development of the concept concerning primary colloidal–disperse ore-forming systems; this concept has been published previously only as abstracts (Safonov, 2003, 2004a, 2004b).

OVERVIEW OF THE CONCEPTS ON GOLD MINERALIZATION IN THE WITWATERSRAND BASIN

The geology and gold mineralization of the Witwatersrand Basin and the history of its discovery and development, including the last decades, were reviewed by Frimmel et al. (2005) on the basis of original investigations and a survey of the literature. We focus our attention on the topics outlined above with allowance for insufficient knowledge of Russian geologists on the current genetic concepts concerning the world's most unique ore-bearing (Au, U, Os–Ir) basin. Almost 50 kt of gold was mined out over the 120 years that "conglomerates" of the Witwatersrand Basin have been an object of mining. The retained reserves within a depth interval of 3.5–4.0 km are estimated now at 40 kt. The results of drilling and geophysical survey indicate that ore-bearing units occur at a depth of 5–6 km. Their discovery, together with the available information on a great amount of subeconomic ore, suggests that the current gold resources of the basin obviously exceed 100 kt. Despite the fact that gold orebodies are mostly blind, their localization has been studied in detail owing to numerous boreholes and underground workings, as well as to geophysical survey within goldfields and beyond their limits.

Since the gold concentrations in the Witwatersrand Basin are unique, the terminology that pertains to the spatial distribution and genetic features of ore mineralization requires some comment. The basin as a whole may be regarded as an ore (metallogenic) province. If the basin is outlined according to the occurrence of the Witwatersrand Supergroup, its length in the northeastern direction amounts to 350 km at a width of 200 km in the southwest and 80 km in the northeast (Fig. 1). The presented sketch map demonstrates the occurrence of Neoarchean terrigenous complexes (systems, or groups), overlapped to a considerable extent by volcanic rocks of the Ventersdorp Supergroup, carbonate and terrigenous rocks of the Proterozoic Transvaal System, and Paleozoic platform rocks of the Karoo Group. The major Central Rand Group is about 3 km thick. This thickness approximately equals the maximal thickness of the overlying Ventersdorp Group and is about 1000 m less than the thickness of the underlying West Rand Group, composed of metaterrigenous rocks that overlie metavolcanics and quartzites of the Dominion Group (2.7 km). Some authors regard the latter group as an independent unit, while the others include it in the Witwatersrand Supergroup.

The locally developed Black Reef Formation, as thick as 500 m, is recognized at the base of the carbonate rock complex of the Transvaal System 3.5–4.0 km in total thickness (Coward et al., 1995). The youngest (2.5 Ga) reefs, of the same name, hosted in the basal unit of this formation are mainly localized in the East Rand goldfields and easterly in the Evander goldfield and in some places of the western goldfields. All other reefs reside in the Central Rand Group, 2.90–2.84 Ga in age. The goldfields of the northern limb of the basin, including the Carletonville goldfield, make up a tract more than 100 km long. More than 50 km of this length is made up by the Central Rand goldfield, which extends in the east-southeast direction, merging with the East Rand goldfield. Many Au-bearing reefs located here steeply dip southward in their upper parts and flatten with depth. The Elsburg, Kimberley, and Bird reefs; the Main series of reefs; and Government Reef (listed from younger to older) were mined in the first half of the 20th century. In addition to the aforementioned reefs, some other reefs, both small and significant, are known in this part of the basin; their correlation with the main reefs is hindered by tectonic dislocations, which are especially numerous in the western part of the basin (the West Rand and Welcom goldfields), inferior in the scale of gold mineralization. The West Rand goldfield is a relatively small goldfield, where Au-bearing reefs hosted in the Central Rand Group were mined along with U-bearing reefs (not typical of the basin) localized at the base of the Dominion Group. The large Welcom goldfield is characterized by a complicate arrangement of reefs and differs from other fields in thickness and composition of some units. The Basal Reef, the most important, is correlated by some researchers with the Vaal Reef in the Klerksdorp goldfield (Minter et al., 1986). The Klerksdorp and Carletonville goldfields are characterized by a relatively simple structure. The inclined VCR (the largest reef in both goldfields) and the Kloof, Liebenen, Middelvlei, Carbon Leader (Carletonville), and Vaal (Klerksdorp) reefs occur here overlain by basalts of the Ventersdorp Supergroup and rocks of the lower part of the Transvaal System (shales, dolomites, and volcanics); the Vaal Reef is not thick but is enriched in gold. The mining here reached the record depth of 3.5 km. In total, more than 20 Au-bearing reefs have been mined out in the past or continue to be mined now. Eight to ten reefs that may be regarded as the major ones occupy a certain position in the stratigraphic section and are traceable through several goldfields. However, the correlation of reefs hosted in the Central Rand Group within particular goldfields is not always proved sufficiently. This correlation is founded on the basic genetic model that

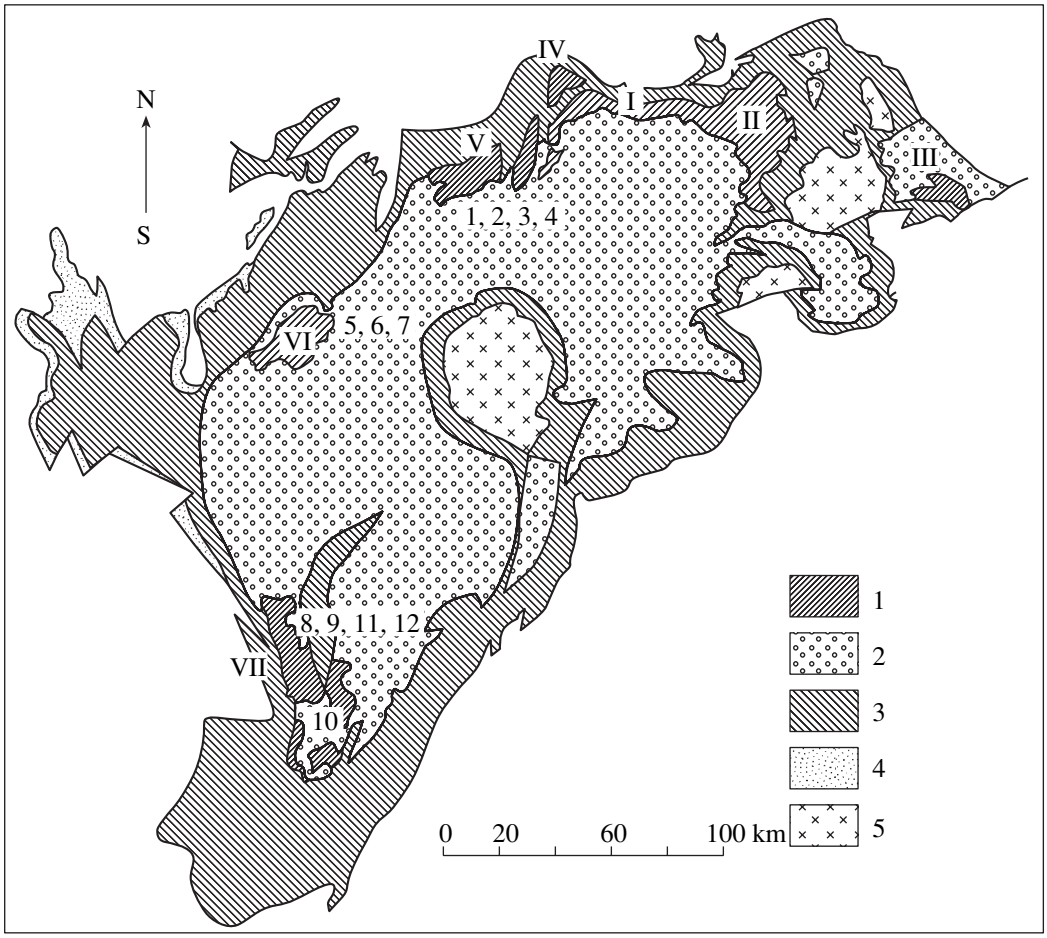

Fig. 1. Sketch map of the main stratigraphic subdivisions in the Witwatersrand Basin: lateral section at the base of the Ventersdorp Supergroup and location of goldfields. Modified after Myers et al. (1990). (1) Goldfields; (2–4) stratigraphic groups: (2) Central Rand, (3) West Rand, (4) Dominion; (5) crystalline basement. Goldfields (Roman numerals in map): (I) Central Rand, (II) East Rand, (III) Evander, (IV) West Rand, (V) Carletonville, (VI) Klerksdorp, (VII) Welcom. Main reefs in the western goldfields (Arabic numerals in map): (1) Ventersdorp Contact, (2) Kloof, (3) Liebenen, (4) Carbon Leader, (5) Black, (6) Ventersdorp Contact West, (7) Vaal, (8) Eldorado, (9) Andenk, (10) Beisa-Beamrix, (11) Basal (Steyn), (12) Commonage.

considers the reefs to be near-shore marine and alluvial (channel fill and bench) placers. However, in some publications, e.g., (Geological…, 1990), it was shown that during certain periods the Witwatersrand Basin developed as a system of subbasins bounded by faults. The appreciably specific sequences of host rocks in goldfields of the northern belt and the western part of the basin, particularly in the Welcom goldfield, and the difference in structure of these fields do not allow even some large reefs to be correlated with confidence.

The Black Reef and VCR, confined to interformational unconformity surfaces, stand out against the other Au-bearing reefs. Each reef combines a series of orebodies that bear the same name but are mined autonomously. The main reefs hosted in the Central Rand Group, often clearly related to interformational unconformities, are contrasted with subordinate reefs, which are occasionally associated with the main reefs. Zones of closely spaced reefs are known, for example, in the Carletonville goldfield near the Ventersdorp Contact and Carbon Leader reefs (Fig. 2). The ore-bearing reefs are stratiform bodies composed of oligomictic conglomerates and arenitic quartzites in various proportions and diverse in mode of occurrence, texture, and composition. The thickness of reefs varies from 10 cm to 3–5 m; orebodies as thick as 10 m and veinletlike "reefs" a few centimeters thick are also noted. Gold commonly occurs as fine and very fine inclusions and veinlets in pyrite (80% total Au) and, to a lesser extent, as free gold of the same fraction (80–100 μm, on average) in quartz cement. A part of larger, including visible, gold grains is related to kerogen–bitumen segregations in close association with uranium minerals and Os–Ir mineralization. These estimates were taken from papers and books published 20–30 years ago. In recent publications, the relative amount of gold related to carbonic substances is considered to be higher. According to the available information, the Au grade of orebodies

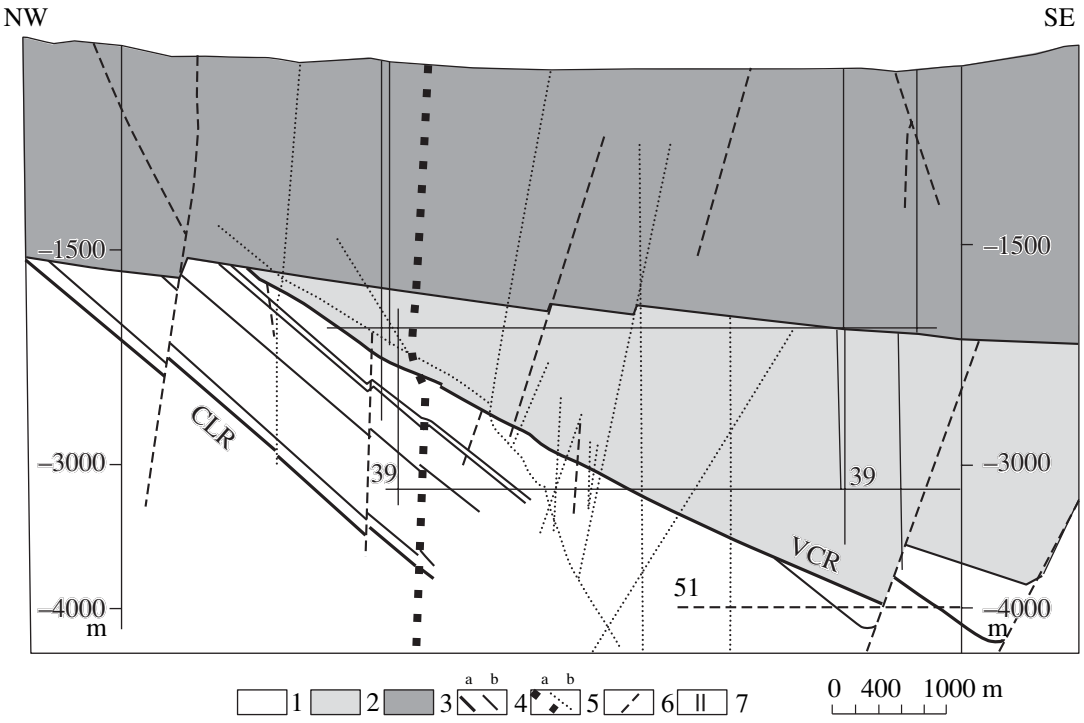

Fig. 2. Geological section of an area at the Kloof Mine, West Wits Line goldfield, after the Geological Survey of the Anglogold Company. (1) Terrigenous rocks of the Central Rand Group; (2) Kliprieversberg Volcanics of the Ventersdorp Supergroup; (3) rocks of the Transvaal Supergroup; (4) ore-bearing reefs: (a) major (VCR, Ventersdorp Contact; CLR, Carbon Leader), (b) subordinate; (5) dikes: (a) thick and (b) thin; (6) faults; (7) mine shaft; horizontal solid lines are mining levels and their numbers; dashed lines are developed levels; the outermost vertical lines are boundaries of the mining lease and depth marks.

is commonly measured as a few tens of grams per ton. This grade may be provided by an interlayer 1 cm thick with anomalous Au content (thousands of grams per ton) and by more uniform Au distribution throughout the mining unit (about 1 m thick).

The total mass of gold in particular reefs varies in a wide range and, according to approximate estimates, amounts to hundreds or thousands of tons.

Advocates of primary placers explain differences in ore mineralization and mode of occurrence of ore-bearing conglomerates by facies conditions of near-shore marine and alluvial (channel–terrace) sedimentation (Myers et al., 1990; Minter and Loen, 1991). The elevated Au grade of channel facies is noted. The Au and U grades decrease on moving away from the shoreline, and the composition of reefs changes in the same direction. The enrichment of some reefs in gold is regarded as a result of uplifting and scouring of previously formed reefs. For example, the formation of the Black Reef in the eastern goldfields might be explained by erosion of the Kimberley Reef, but such an interpretation was not generally accepted. Various versions of the genetic model of metamorphosed (modified) placers assume that Au grades are generally retained at the primary level without significant migration of gold. Recent variants of this model that are referred to as small-scale (range) modification (redistribution) models emphasize only an insignificant contribution of metamorphism to the formation of ore concentrations in the basin even in their names (Frimmel et al., 2005). The concept of modified placers suggests that the offshore Paleo- and Mesoarchean (3400–3000 Ma) greenstone belts served as sources of gold.

The most vulnerable link in the genetic model of placers related to offshore sources is the high primary Au grade and uniform composition of placers within a great depth interval that embraces more than five kilometers. The theory and practice of placer geology (Shilo, 2002, and many others) indicate that placers related to distant sources fix much less than 50% of the gold initially contained in the eroded deposits. If even 50% is accepted as a limit, the inferred provenances should have contained tens of thousand of tons of gold and more than 200 kt Au in total.

It is known that, in the largest Archean Au-bearing belts (Abitibi in Canada and Yilgarn in Australia), the mined gold and its potential resources are estimated at 5–10 kt in each belt and the largest deposits contain as much as 2 kt Au (Card et al., 1989; Woodal, 1990). The world's largest goldfields—Muruntau and Grasberg—contain 4–5 kt Au as primary resources. No indications of ore-forming systems of the same or a higher productivity have been revealed in Archean Au-bearing belts, including the Barberton greenstone belt and other areas that surround the Witwatersrand Basin.

Only one large Mesoarchean gold deposit, Bag Bill in western Australia (3 Ga in age and with resources of 100 t Au), is known to date. No larger eroded or hidden deposits in ancient cratons have been reported. The certain similarity in mineral composition and geochemistry of ore from greenstone belts and reefs of the Witwatersrand Basin (Hutchinson, 1987), when considered in detail, does not support a common character of placer-forming mineral assemblages or the possibility of formation of such uniform detrital heavy mineral fractions as are ubiquitous throughout the Witwatersrand Basin (pyrite, gold, chromite, Co, Ni, and Os–Ir minerals) even under conditions of a reducing atmosphere. Granitic complexes are commonly accepted as sources of uranium mineralization. It should also be noted that, in the case of erosion of hypo- and mesothermal gold deposits at Archean cratons, a common feature of the mineralogy of these deposits must be inherited by gold passing into placers, namely, elevated gold contents in the upper part of the 2- to 3-km vertical interval of ore mineralization. The Au grade and thickness of orebodies decrease with depth. The mineral composition of gold–quartz deposits becomes simpler with depth as well. At the Kolar gold deposit in India, as one of the most spectacular examples of gold mineralization hosted in greenstone belts, this zoning is clearly expressed within a vertical interval of 3100 m, where the Au grade decreases downward from 30–40 to 3–5 g/t, while the thickness of orebodies is reduced from 2–20 to 0.2–0.5 m, along with substantial textural variation of quartz.

Taking the zoning of the Archean primary deposits into account, one may expect that the lower part of the conglomerate complex, as a placer related to distant sources, must be enriched in detrital gold. No significant Au-bearing reefs were found in the West Rand and Dominion groups of the Witwatersrand Basin. The lower part of the main ore-bearing Central Rand Group does not show the enrichment of reefs in gold either. These relationships are used as arguments in favor of an alternative model, the hydrothermal replacement model, developed by Phillips and Law and their colleagues (Phillips et al., 1989, 1997; Law et al., 1990; Law and Phillips, 2005). It is suggested that metamorphic fluids are enriched in gold owing to its leaching from the underlying complexes. However, no reliable data can be adduced confirming that such a process actually took place.

A model of exhalation–sedimentary deposition of gold and a part of pyrite was proposed by Hutchinson and Viljoen (1988). Accepting different sources of gold, a placer nature of uranium minerals, and an important contribution of metamorphism to the redistribution of ore components in reefs, this model opened new paths to the interpretation of formation conditions of reefs in the Witwatersrand Basin and their polygenetic character.

Shcheglov (1994), having studied the ore in the Witwatersrand Basin and surveyed the previously published data, arrived at the conclusion of a polygenetic sedimentary–hydrothermal and metamorphic origin of the Witwatersrand gold deposits. Some researchers (Konstantinov, 1991; Kremenetsky and Iordan, 1996; Kremenetsky et al., 1997) regarded the reefs of the Witwatersrand Basin as products of a sedimentary–hydrothermal process. These views replaced the ideas of the placer origin of these reefs that were popular previously among Russian geologists (Krendelev, 1974).

Shilo and Sakharova (1988) showed that no pyrite pebbles of alluvial origin occur in the Witwatersrand paleoplacers. In the opinion of Shcheglov, pyrite and quartz pebbles could have become rounded in gaseous hydrothermal ore-bearing flows that were supplied to the aqueous medium simultaneously with formation of conglomerates. Like Portnov (1988), Shcheglov most likely took into account the data reported by Genkin et al. (1980), who suggested the formation of rounded pyrite clots in explosion breccia at the Kochbulak epithermal deposit. Later on, this idea was reconsidered (Safonov and Kassim, 2002; Safonov, 2003, 2004). Additional study showed that pyrite morphology depends on the transition of colloidal solutions to true ones and their inversion with formation of various rounded pyrite segregations.

Shcheglov (1994) inferred that a part of quartz "pebbles" in reefs of the Witwatersrand Basin were formed as a result of coagulation and coacervation of silica gels in the aqueous medium due to supply of ore-bearing hydrothermal solutions. It should be noted that such terms as *gel, colloform morphology, nodules*, and *concretions* are sporadically met in early publications of South African researchers in characterization of pyrite segregations. At the same time, Shcheglov and some Russian (Tsarev, 1990, 2002) and other foreign authors developed the idea of a metasomatic origin of the rounded pyrite segregations replacing magnetite and quartz "pebbles" formed by replacement of lithic pebbles initially composed of host rocks. In the opinion of Shcheglov, the ore-bearing hydrothermal solutions were derived from the mantle. He classified uranium minerals and presumably a part of gold in conglomerate as sedimentary in origin. While reasoning on the possibility of epigenetic hydrothermal formation of gold mineralization, Shcheglov adduced facts that come into conflict with this suggestion.

STRUCTURE AND COMPOSITION OF Au-BEARING REEFS

The collected samples, along with observation in underground mines and at the Earth's surface, are believed to be sufficient for evaluating the published information on common and different features of reefs in the Witwatersrand Basin and for assurance that reported characteristics (Anhaeusser and Maske, 1986, etc.) are not accidental.

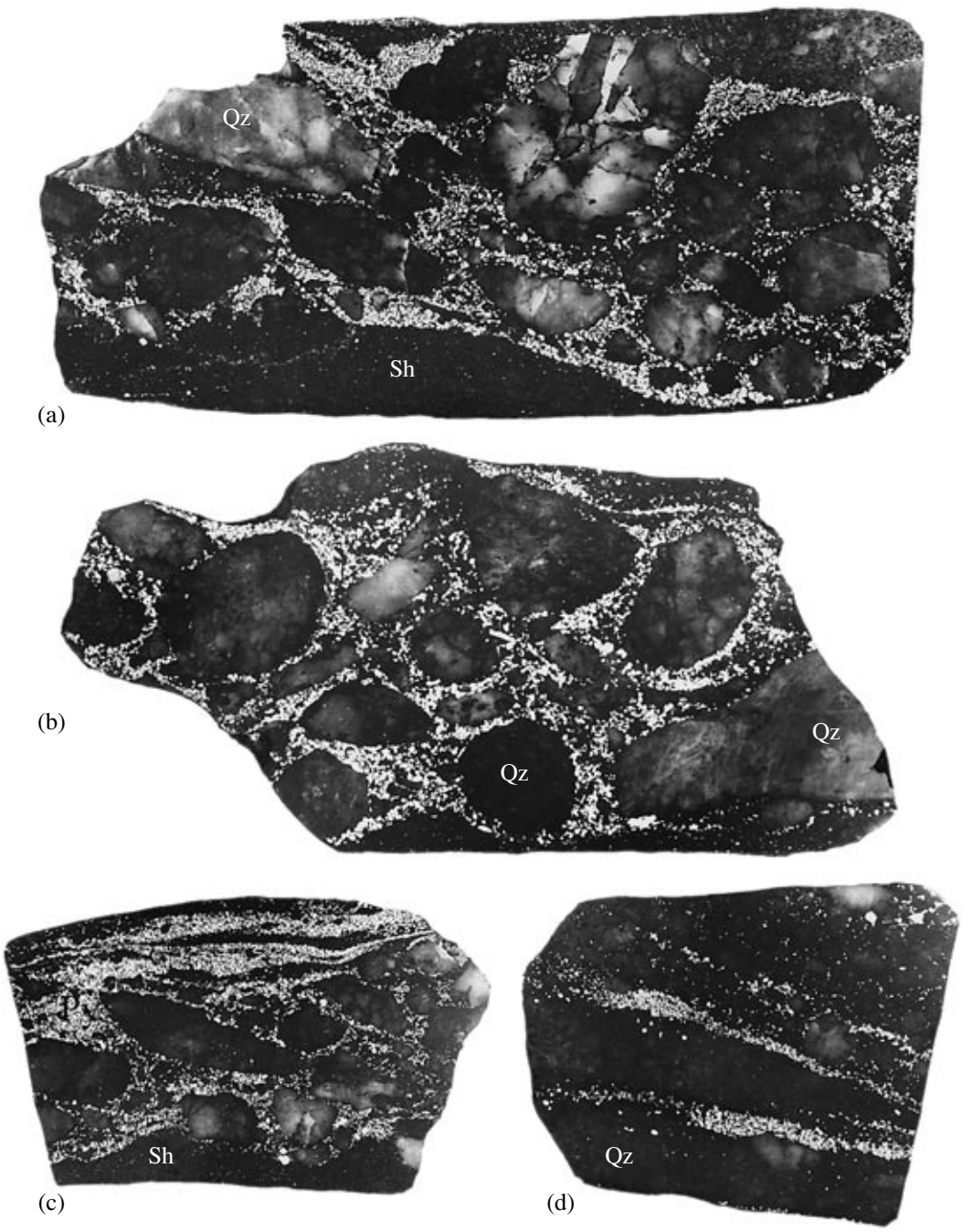

Fig. 3. Textures of ore from the Black Reef. Photos of polished hand specimens in reflected light. (Py) pyrite, (Qz) quartz, (Sh) shale. Size of the lower sides of hand specimens, cm: (a) 12.5, (b) 7, (c) 6.5, and (d) 5.

The Black Reef in the examined open pit is a near-horizontal bed of black shale overlain by a unit of gray dolomite more than 100 m in apparent thickness. The contact between shale and dolomite is sharp and slightly tortuous. The rocks of the reef are foliated; small-amplitude folds developed locally are generally controlled by nearly conformable foliation. A quartz boulder and pebble conglomerate as a stratiform body with complicate vague contacts with shale occurs in the lower portion of the bed at a distance of 1.0–1.5 m from the contact with dolomite. The boundaries of the "conglomerate" reef in some places are vague and established only by the position of quartz pebbles and veinlets and segregations of pyrite related to the foliation planes (Figs. 3a, 3b). The latter control veinlets and zones densely impregnated with pyrite, which occupies more than 20% of the volume of the material that cements "pebbles." The thickness of the pyrite–quartz

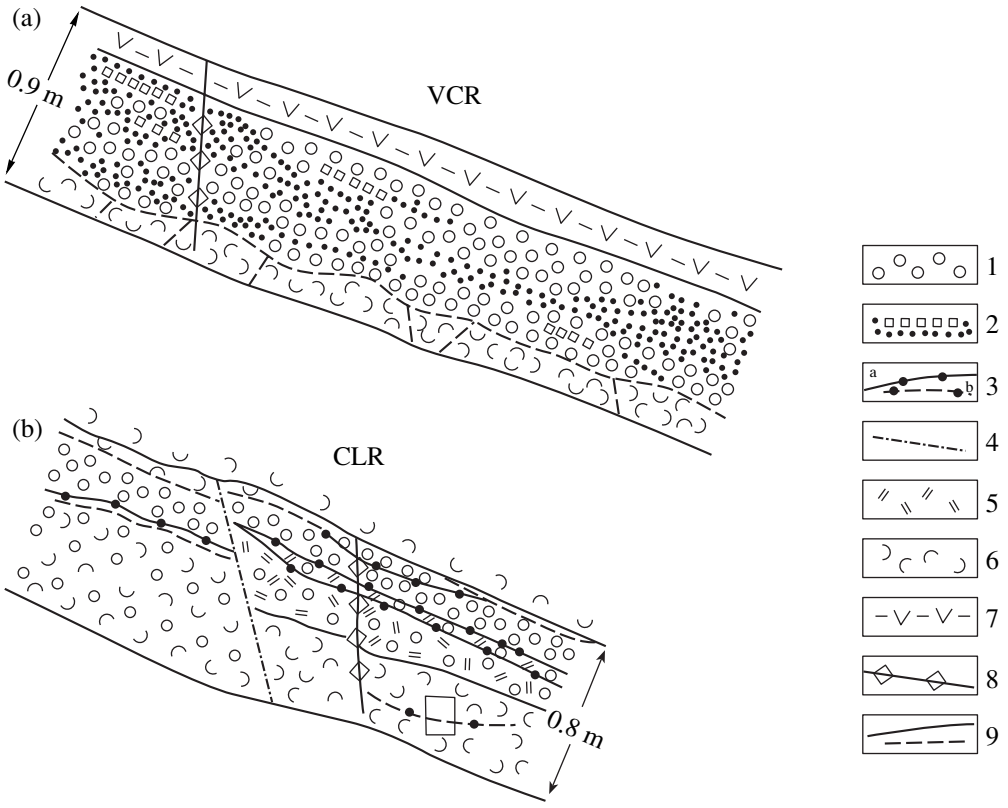

Fig. 4. Internal structure of the (a) Ventersdorp Contact and (b) Carbon Leader reefs (documentation of breakage heading walls). (1) "Conglomerates" (reefs), (2) pyrite veinlets and pockets in quartz mass, (3a) kerogen–bitumen and (3b) kerogen–carbonate veinlets, (4) fractures, (5) zone of disseminated organic matter, (6) quartzite, (7) basaltic andesite and basalt, (8) quartz veinlets, (9) sharp upper and poorly expressed lower boundaries of reef. The rectangle indicates the location of samples.

body over 100 m along the strike varies from 0.5 to 1.0–1.5 m. The pyrite veinlets are largely oriented nearly concordantly or obliquely to the bed and contacts of oblong "pebbles." In severely foliated segments, such "pebbles" resemble quartz boudins within the deformed shales with distinct slickensides at graphite-like planes (Figs. 3c, 3d).

As has been shown by many researchers, the Black Reef does not differ in mineral composition from other reefs hosted in the main ore-bearing Central Rand Group. In addition to enrichment in carbonic matter, this reef is characterized by elevated Os and Ir contents. The anomalously abundant carbonic matter, which is dispersed through the rock, fills microfractures in quartz pebbles, and occurs in cement, is a specific feature of the Black Reef in contrast to the Kimberley Reef, which is overlapped with a sharp angular unconformity by the Black Reef shale near the open pit. The Kimberley Reef is penetrated here by boreholes and is more than 5 m thick. White, gray, and black quartz, sandstone, and shale pebbles are incorporated into fine-grained quartz cement; the volumetric proportions of pebbles and cement are variable.

As judged from numerous descriptions, the VCR is the most widespread (more than 500 km^2 in the western part of the basin) and variable in morphology, thickness, and internal structure. This variability is related to the morphology of the unconformity surface, the effect of overlying basaltic lavas on incompletely lithified sediments, and tectonic dislocations. The same factors are reflected in the internal structure of the Au-bearing reef, which should more likely be regarded as a series of orebodies contoured by economic Au grades.

Judging from the available descriptions, the VCR in the observed underground mines of the Carletonville goldfield does not show any difference from its other sections at deep levels. The conglomerate unit is 70–100 cm thick (Fig. 4a) and composed of fine-pebble conglomerate with pebbles (1–3 cm) of white-gray quartz and contrastingly distinguished rare pebbles of black and dark gray quartz. Pyrite veinlets are commonly oriented downdip the unit (~20°) and locally controlled by fractures. Organic matter is dispersed largely through the cement as fine disseminations. Small crosscutting veinlets of white quartz are observed. The outer characteristics of this reef correspond to Green VCR. The Geological Survey of the West Wits Line mines recognizes eight other varieties of this reef (black, poorly sorted, etc.) distinct in color of cement and degree of clastic material sorting. The green color is caused by abundant sericite with a chrome admixture. The samples from the Doornfontein

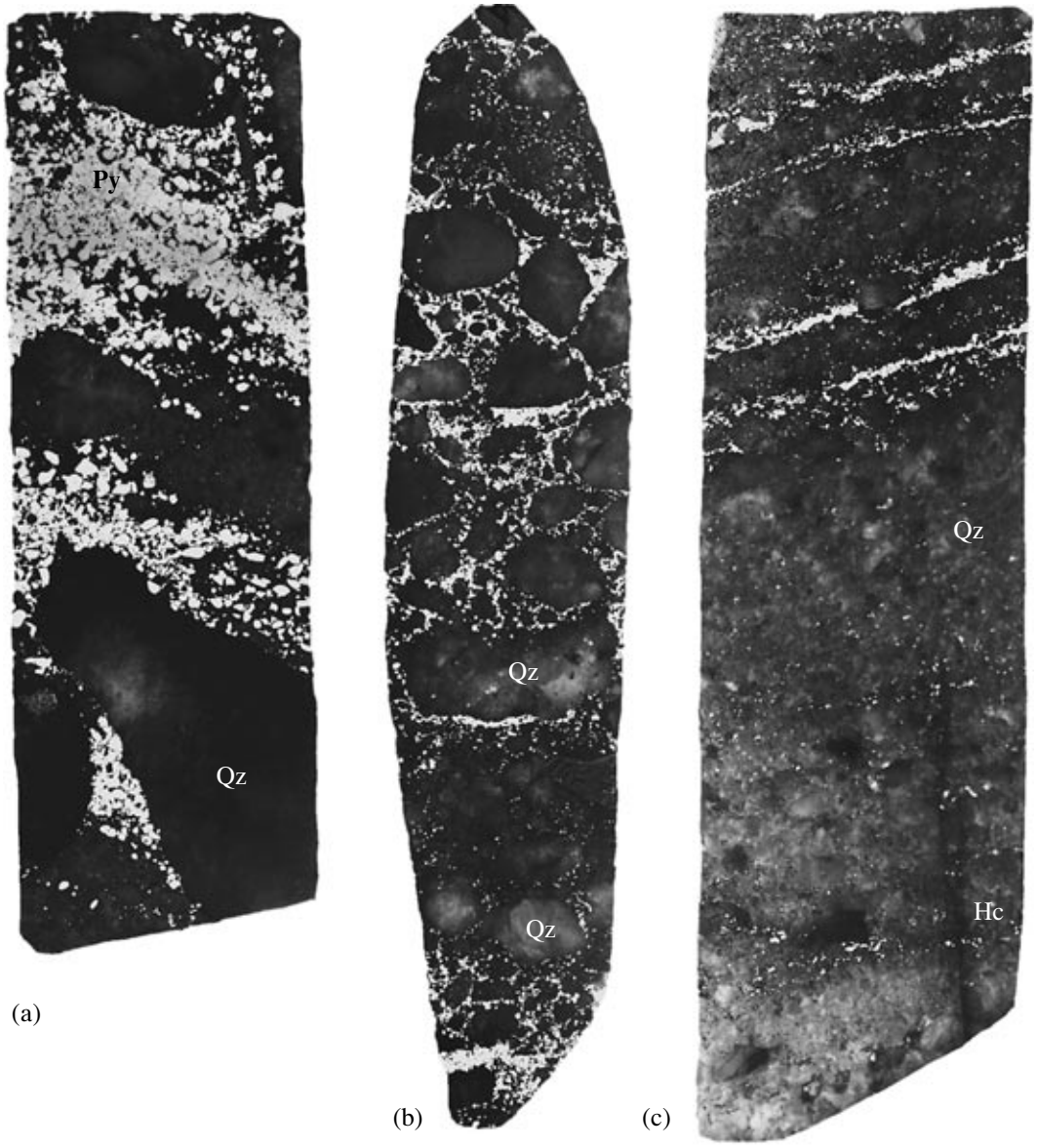

Fig. 5. Textures of ore from the (a) Ventersdorp Contact and (b, c) Carbon Leader reefs. Photos of polished hand specimens in reflected light. (Py) pyrite, (Qz) quartz, (Hc) kerogen–bitumen matter. Size of the right sides of hand specimens, cm: (a) 9.3, (b) 8, and (c) 10.5.

Mine, Green VCR, are distinguished by widespread pyrrhotite as grains, veinlets, and pockets together with an obviously subordinate abundance of pyrite. In the observed Deelkraal Mine, sericite–quartz aggregates in the reef make up separate zones 2–5 cm or more in thickness. Pyrrhotite occurs within these zones as disseminations and crosscutting veinlets. Large quartz pebbles and pyrite segregations are typical of the VCR at the Kloof Mine (Fig. 5a).

The Carbon Leader Reef in the observed mines does not look like a conglomerate unit. Pebbles are distinguished here only conditionally within vague zones varying in thickness from 1–2 to 30 cm and having a brecciated structure (Fig. 5b). Large (about 1 cm in diameter) quartz segregations within these zones are difficult to distinguish from the cementing fine-grained quartz mass. At the same time, nearly concordant slightly tortuous veinlets of carbonic matter are traced distinctly (Fig. 4b). As can be seen from the sketch, the veinlets in the central zone of the "pebble" layer are distinguished by a greater thickness and crosscut by thin quartz veinlets. A carbonate veinlet with dispersed carbonic matter was found at the footwall of the reef, where it is hosted in light quartzite that contains pyrite and carbon disseminations. The pyrite veinlets in the quartzite footwall differ from the thicker and more concentrated veinlets in the central zone of the reef (Fig. 5c). As is pointed out in publications, the Carbon Leader

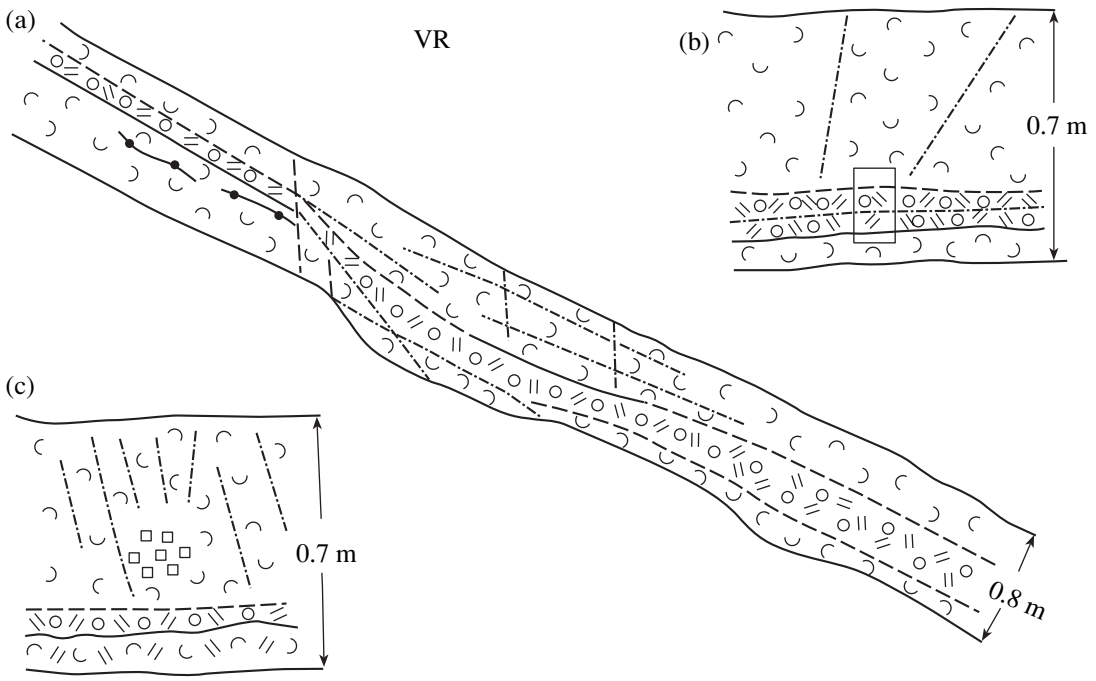

Fig. 6. Internal structure of the Vaal Reef. (a) Documentation of a breakage face; (b, c) documentation of sublevel headings. See Fig. 4 for legend.

Reef stands out due to elevated Au and U contents and local PGE concentrations. By the middle of 1979, 3164 t Au and more than 9 kt U had been mined out at average grades of 20.9 g/t Au and 150 g/t U. By that time, 1330 t Au had been recovered from ore with a grade of 15 g/t Au mined out from the VCR (Engelbrecht et al., 1986).

The Vaal Reef, which is documented in the breakage headings of the Kopanang Mine as a contrasting dark gray thin bed (Fig. 6) consisting of grained quartz and carbonic matter with pyrite disseminations, is characterized by elevated Au and U contents as well. Segregations and veinlets of crystalline pyrite occur in quartzite and only sporadically in the U- and Au-bearing unit itself. Both concordant and crosscutting fractures, occasionally accompanied with gouge, are typical. Similar fractures are observed along the bed contacts. Thin basal layers of carbonic matter with visible gold are also controlled by fractures. The Au grade in such layers amounts to 750 g/t against 30 g/t in the reef, on average (Antrobus, 1986). Since publications by Schidlovski (1981), Hallbauer (1981), and other authors, the carbon layer at the base of the conglomerate unit is perceived by many researchers as an obligatory attribute of ore-bearing reefs. More likely, this is one of the modes of occurrence of kerogen–bitumen material difficult to distinguish from veinlets, which are also confined to contact surfaces and control columnar aggregates of carbonic matter.

According to the published data, 70–100 minerals have been identified in ore-bearing reefs of the Witwatersrand Basin. Quartz; pyrite; native gold; pyrrhotite; chalcopyrite; As, Co, and Ni sulfides; native silver; uraninite; brannerite; galena; chromite; zircon; and ilmenite are major minerals; the gangue minerals comprise sericite, chlorite, pyrophyllite, chloritoid, and biotite. Thucholite is the most well-known mineral species of carbonic matter; in the opinion of some researchers, the abundance of this mineral is overestimated. Appreciable Th contents in carbonic matter are rare.

The major minerals of U- and Au-bearing reefs were described first by Ramdohr (1958). Later on, this list was confirmed and supplemented by other researchers (Hallbauer, 1981, 1986; Saager, 1981; Saager et al., 1982; etc.). Most of these minerals were identified in the samples taken by the authors of this paper. Pyrite is the most abundant ore mineral; its average content in the reefs was previously estimated at 10% and subsequently reduced to 3–5%.

As was mentioned above (Fig. 3), the "conglomerate" unit of the Black Reef contains more than 20% pyrite. The veinlets and breccia ore are the most expressive here. Pyrite veinlets occur in the country shale as well. Pyrite segregations in quartz pebbles occasionally resemble massive material. Dense pyrite impregnation is detectable in the samples from the VCR at the Kloof Mine, whereas, in the observed underground workings in this reef, as well as in the Carbon Leader Reef, the pyrite content is lower and the ore texture is largely stringer–disseminated and brecciated (Fig. 5).

Pyrite attracted the most attention from researchers. This mineral was classified by Ramdohr into pebble-shaped, pseudomorphous, concretionary, and hydro-

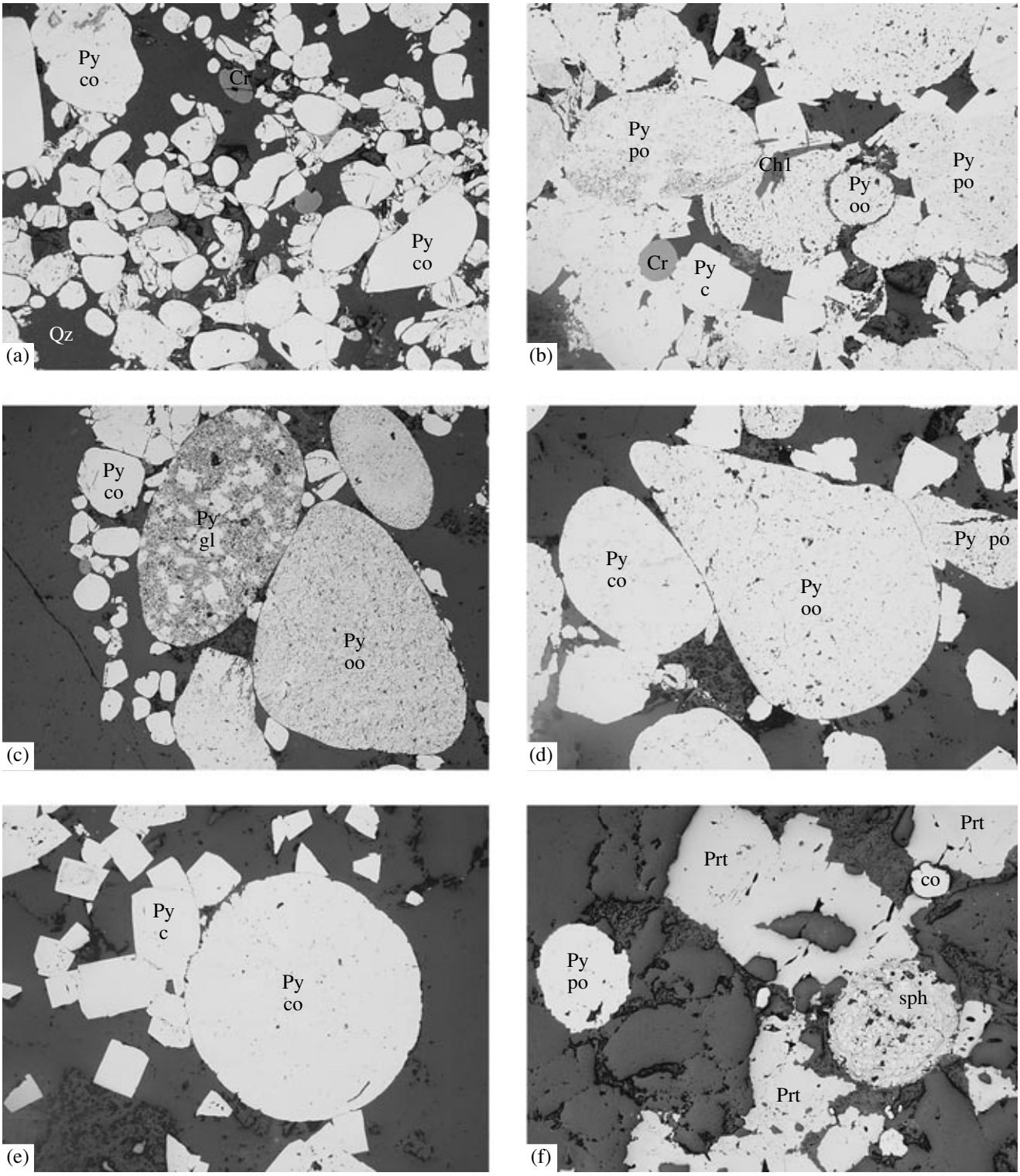

Fig. 7. Morphological types of pyrites from the (a) Carbon Leader Reef and (b–f) VCR. Photos of polished hand specimens in reflected light (here and hereafter). Horizontal width (mm): (a–d) 2.6; (e, f) 1.3. (a) Predominant rounded compact pyrite (Py) in association with split compact (co) and porous (po) pyrite and chromite (Cr); (b–d) assemblages of compact (co), globular (gl), concretionary (cc), oolitic (oo), and porous (po) crystalline (c) pyrite; (Cr) chromite; (Chl) chloritoid; (e) spherical compact (Py co) and crystalline (c) pyrite; (f) porous (po) compact pyrite and spherulitic (sph) pyrite replaced with pyrrhotite (Prt) incorporated into a sericite–quartz mass.

thermal varieties. Hallbauer (1986) and other authors described the following genetic varieties of pyrite: (i) allogenic detrital; (ii) synsedimentation; (iii) pseudomorphs and replacements; (iv) authigenic postsedimentation; and (v) late hydrothermal and pseudohydrothermal. Saager (1981) recognized only three genetic varieties of pyrite: (i) rounded compact pyrite of detrital origin; (ii) concretionary or porous, occasionally "bedded" pyrite, detrital or authigenic; and (iii) pyrite altered during or after metamorphism. Hirdes (1979), who studied the pyrite mineralization of the Kimberley Reef in the Evander goldfield in detail, classified this mineral as (i) authigenic secondary pyrite as a product of diagenesis or metamorphism, (ii) allogenic compact pyrite derived from Archean rocks, and (iii) allogenic porous pyrite derived from sulfide gels or pyrite muds in the Witwatersrand Basin (cited from Tweedie, 1986). Typical examples of the pyrite varieties listed above are shown in Fig. 7. The specific mineralogical features of reefs and their particular segments are determined, to a great extent, by the total amount of pyrite and relationships between morphological varieties. It is deemed that the "pebble-shaped" ("authigenic") pyrite, which is often called "rounded," is the most abundant. However, as follows from illustrations presented in many publications, the percentage of pyrite with rounded outlines that is classified with this generation with confidence is variable. Rounded pyrites are often defined as compact (after Saager) quite arbitrarily. In many cases, such pyrites are porous to some extent, and in other cases, they resemble concretionary varieties. The rounded pyrites—both compact and concretionary—are called buckshot (the local name). Pyrites from the Black Reef are the most peculiar; their relatively large segregations are often defined as a porous, mudball-type variety (Fig. 8). Pyrites from the Black Reef vary in the degree of their roundness and the amount of relict microinclusions of the host matrix. In our samples, compact pure pyrites are observed rarely. They were identified in small orebodies in the Klerksdorp goldfield (Antrobus et al., 1986) and the Evander goldfield, where compact and concretionary pyrites were studied by Barton and Hallbauer (1996). This study showed that these generations of pyrite differ in contents of radiogenic lead.

In our samples, the widest range of morphological and structural varieties of rounded pyrite was established in the VCR. The aggregative segregations of pyrites related to different generations are the most representative in precisely these samples. As can be seen under a microscope, compact pyrite often comes in immediate contact with concretionary pyrite. In some cases, the former exhibits a transitional zone of microfracturing with disintegration into fragments similar in size to concretionary globules. The morphology of some grains of concretionary (porous) pyrite is controlled by contact surfaces of neighboring grains of compact and spherulitic pyrite. Oblong segregations with a variable degree of roundness up to fragments close to a rectangular shape are rather numerous. The typical pyrite spherulites, a few millimeters in diameter (rarely larger), are commensurable with grains of compact pyrite, which occasionally reach 2–3 mm in size against the 0.5- to 1.0-mm-sized grains that are most abundant in this reef (Figs. 7b, 7d).

In the Carbon Leader and Vaal reefs, such pyrites commonly reach fractions of a millimeter in size (Fig. 7a). The quartz "pebbles" occasionally exceed a few centimeters, whereas, in the VCR, the pebbles' size reaches 5–7 cm along the greater axis. Pyrite rims and segregations of pyrite disseminations around quartz "pebbles" (actually quartz fragments 1–2 cm in size) are observed in the Carbon Leader Reef, making up a brecciated texture.

According to our observations, the amount of pyrite in the Carbon Leader and Vaal reefs is not great. Small pyrite grains of various shapes, more often irregular and poorly crystallized, but occasionally skeletal, occur in pyrite–quartz segregations. The sharp contacts of such rounded and elliptical segregations allow us to regard them as metacolloidal in origin.

Separate pyrite crystals are not abundant. Commonly, such crystals are scattered in pyrite aggregates of other generations. A veinlet of crystalline pyrite was found in the middle part of the Vaal Reef. This veinlet is 1.5 cm thick and extends for 10 cm along the strike and down the dip, having an obtuse pinch-out. Pyrite occupies 80% of the veinlet volume.

The reefs are also distinguished by content and mode of occurrence of carbonic matter and minerals belonging to the late sulfide assemblage, as well as by the degree of their resemblance to pebble conglomerate. These features are crucial for understanding the formation mechanisms of ore-bearing reefs (see below).

In the examined polished sections, native gold was revealed as inclusions in compact pyrite (Fig. 9a), as well as in quartz associated with pyrite, porous pyrite, pyrrhotite, and carbonic matter (Fig. 9b). The relation of gold to lamellar pyrite formed as a result of splitting of compact pyrite is notable (Figs. 9c, 9d). Gold in association with pyrite is typical of the VCR, whereas, in polished sections from the Carbon Leader and Vaal reefs, native gold is associated with kerogen–bitumen. The visible gold observed in these reefs is localized in veinlets of carbonic matter and in its columnar segregations within thin interlayers at the lower contact of the reef. The highest gold content was noted in a polished section from the Basal Reef (Welcom), where carbonic matter occurs as a veinlet (layer?) about 1 cm thick. Gold is localized here at the contact of carbonic matter with quartz, in kerogen microveinlets that cross aggregative kerogen, and as disseminations within the latter.

It should be noted that sulfides are not abundant in "massive" kerogen–bitumen segregations. Such segregations in the sulfide–quartz mineral mass of reefs largely occur as small pockets, microveinlets, and ovoid and irregular clots in association with late pyrite

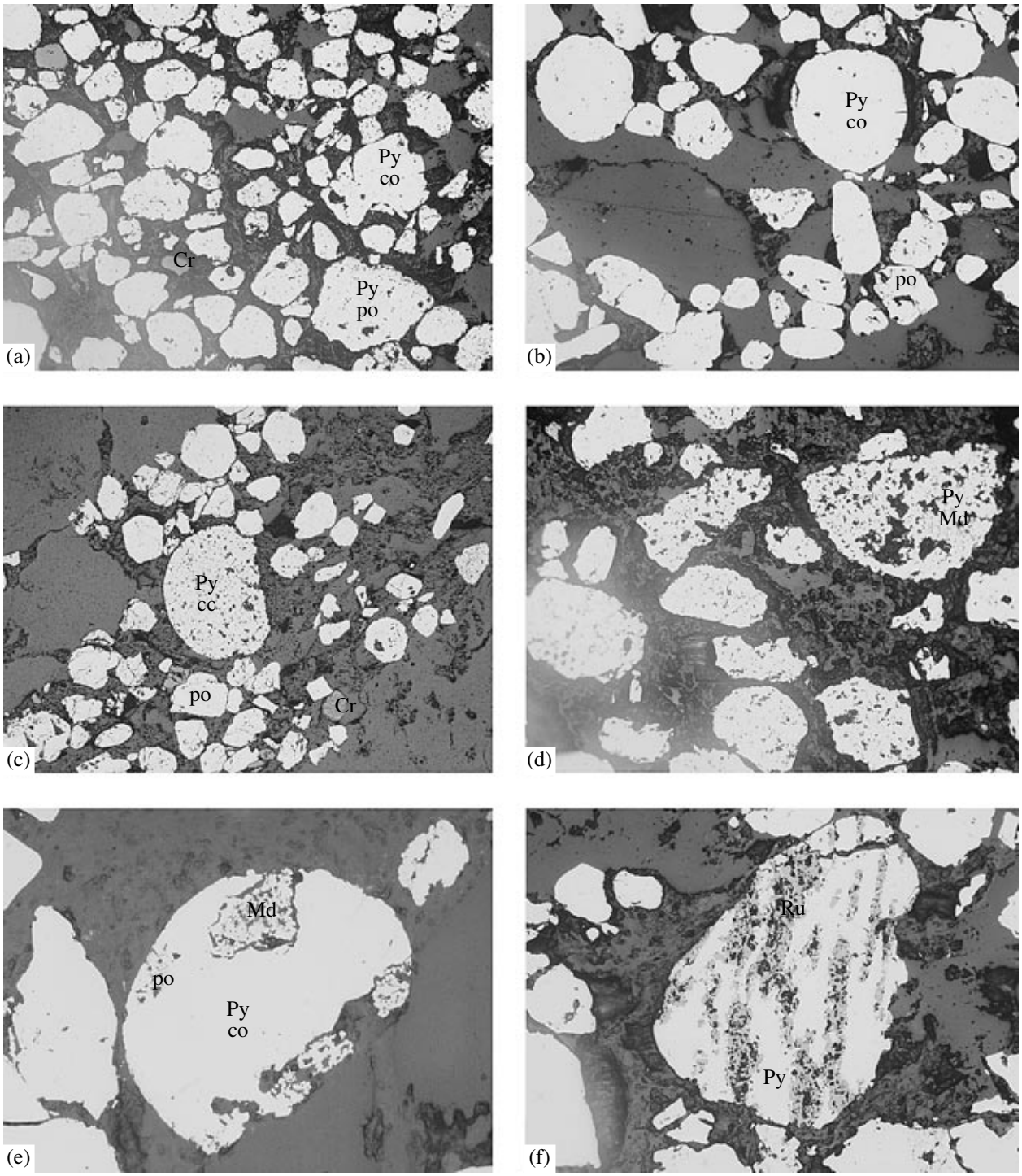

Fig. 8. Typical pyrite segregations in the Black Reef. Polished sections. Horizontal width (mm): (a–c) 2.6; (d–f)1.3. (a) Porous (po) and compact (co) pyrite and chromite (Cr); (b) compact (co) and subordinate porous (po) pyrite; (c) concretionary (cc) and porous (po) pyrite; (d) pyrite of mudball (Md) type; (e) compact (co) pyrite with fragments of partially replaced porous (po) and mudball-type (Md) pyrite; (f) rutile (Ru)–pyrite (Py) intergrowths.

and pyrrhotite, chalcopyrite, and brannerite formed approximately at the same time (Figs. 10a, 10b). Segregated kerogen ovoids and rims around grains of quartz and other minerals are typical.

Pyrrotite, chalcopyrite, and less frequently sphalerite and galena replace pyrites of all generations, including pyrite spherulites. The late sulfide assemblage, mostly without carbonic phases, is developed in various

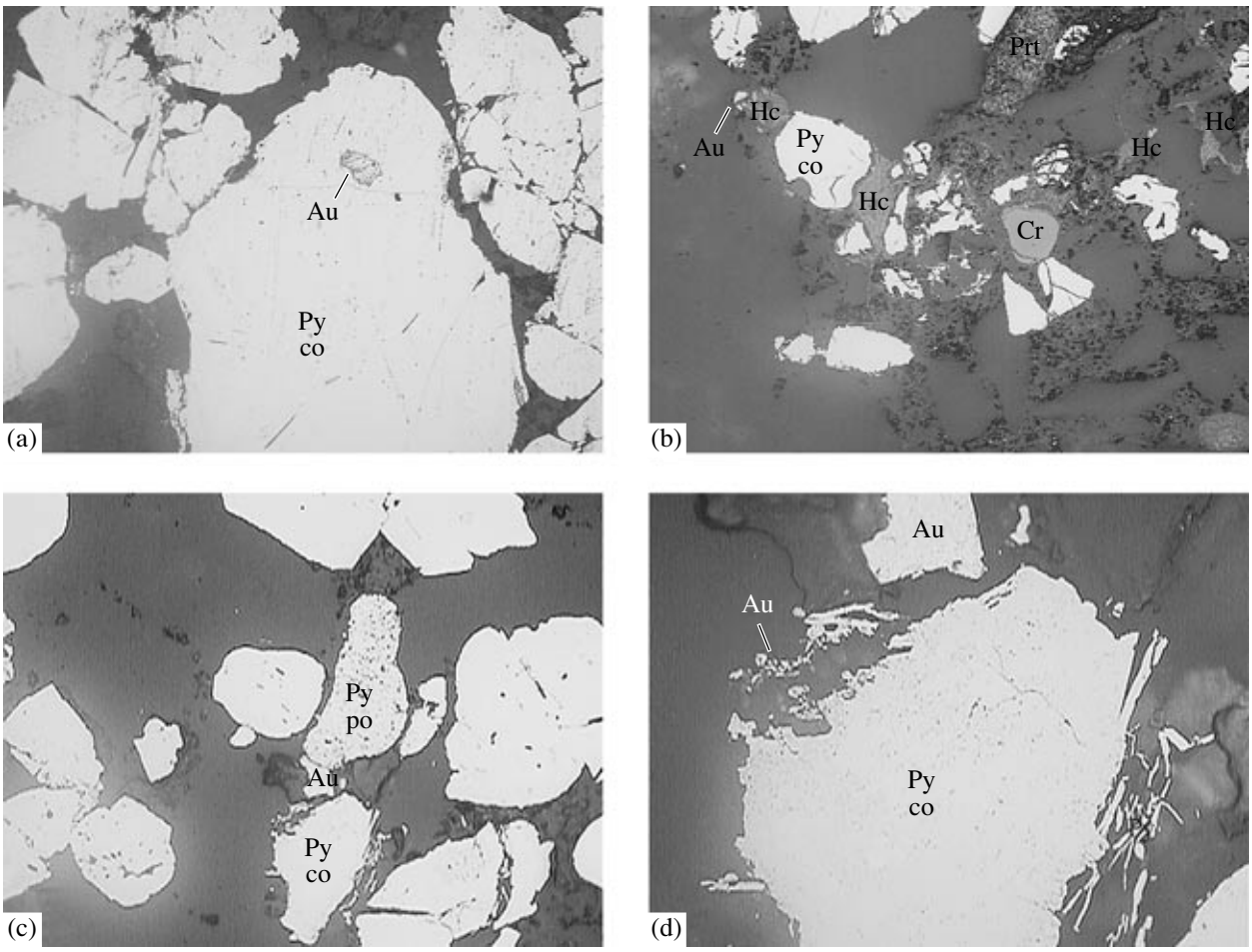

Fig. 9. Gold grains in the (a, c, d) Ventersdorp Contact and (b) Carbon Leader reefs. Polished sections. Horizontal width (mm): (a, c) 1.3; (b) 0.65; (d) 0.325. (a) Gold (Au) grain in corroded compact pyrite (Py co); (b) association of pyrite (Py co), chromite (Cr), kerogen–bitumen (Hc), pyrrhotite (Prt), and gold (Au); (c) gold (Au) in quartz between grains of porous (Py po) and split compact pyrite (Py co); (d) gold (Au) grains of different size intergrown with pyrite sheets at their left (close-up of panel (c)).

reefs with different intensity and variable proportions of the aforementioned minerals. Pyrrhotite is abundant in Green VCR, where this mineral occurs as rather large grains ($n \times$ mm) and is accompanied locally by chalcopyrite. In the Black Reef, this assemblage is observed as linear microsegregations and isolated grains of sphalerite and less frequent chalcopyrite. These minerals, as well as galena, make up fine disseminations in pyrite.

The pyrite–pyrrhotite–chalcopyrite mineralization with subordinate sphalerite and galena in the contact zone of amygdaloid basalts that overlies the VCR should be noted specially. These basalts belong to the lower Klipriviersberg Group of the Ventersdorp Supergroup. The published data on the petrology and mineralogy of these basalts are scanty. Their affinity to the tholeiitic series; a high degree of crystallinity in some units; massive, porphyritic, and amygdaloid textures; and locally developed agglomerate appearance are noted. We observed massive and amygdaloid basalts and basaltic andesite in the hanging wall of the reef. As follows from microscopic examination, both volcanic rocks are chloritized, sericitized, silicified, and impregnated with pyrite. Especially intense chloritization is typical of basaltic andesite. The coexistence of closely spaced amygdules varying from a few millimeters to 1–2 cm across and filled with different minerals attracts attention. Outer rims and segregations of quartz, chalcedony, and frequent chlorite are common. Aggregates of crystalline quartz and chlorite, occasionally with chalcopyrite and pyrite, mainly fill central portions of large amygdules (Figs. 11a, 11b). Numerous microinclusions of allanite and titanite as both isolated disseminations and intergrowths with sulfides, largely with chalcopyrite and less often with pyrrhotite, were detected with an electron microscope (Figs. 11c, 11d). The largest allanite grain (~170 × 80 μm), shown in Fig. 11a, reveals a complex zoning (Fig. 11c) with variable REE contents in separate zones (higher contents in light zones and lower contents in dark zones). The variation in concentration of particular REEs is wide (wt %): 2.63–12.37 La_2O_3, 6.98–14.11 Ce_2O_3, 0.5–1.21

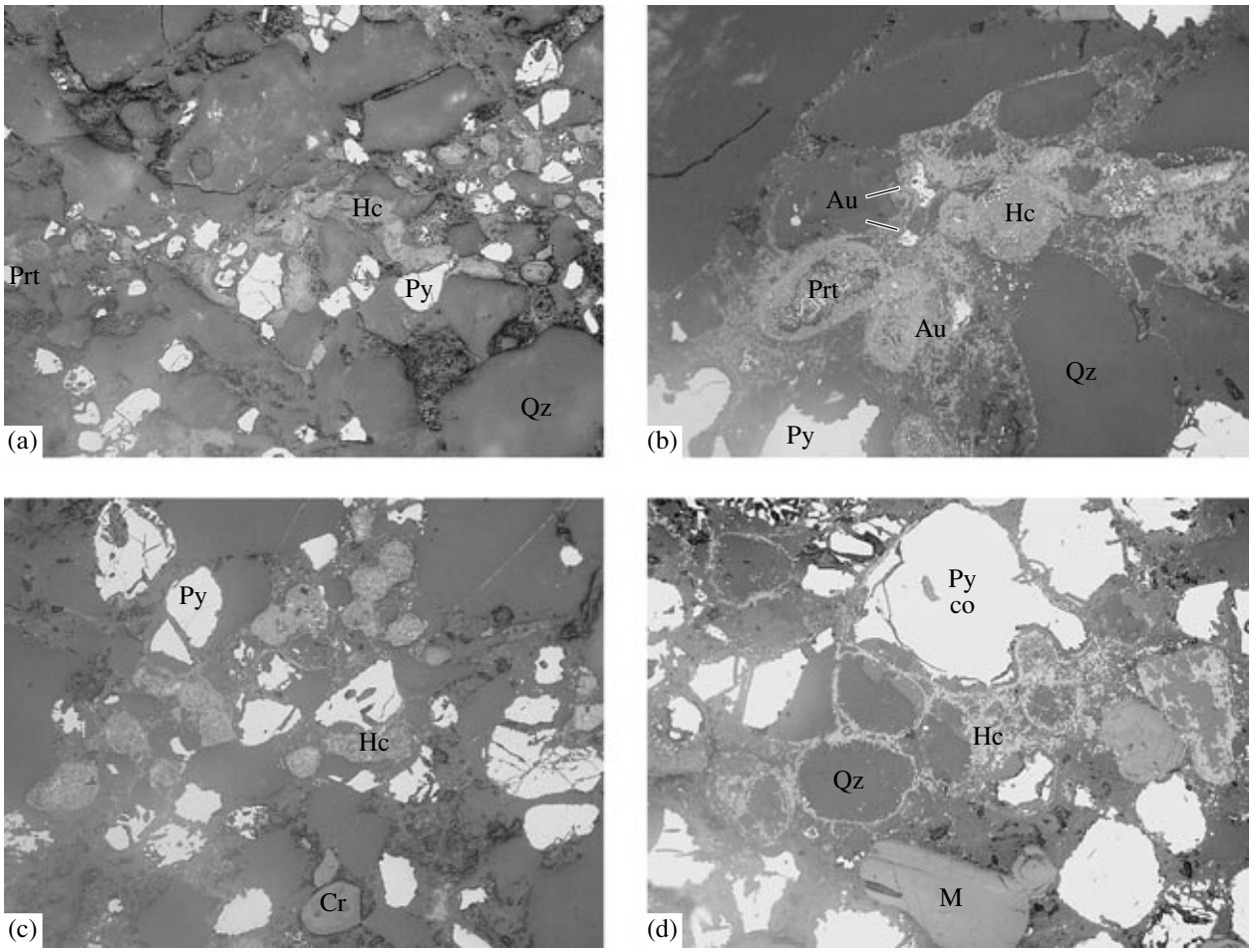

Fig. 10. Kerogen–bitumen (Hc) segregations in a dark gray quartz mass with sericite and chlorite in the (a, b) Vaal and (c, d) Carbon Leader reefs. Polished sections. Horizontal width (mm): (a, c) 2.6; (b) 0.65; (d) 1.3. (a) Framboidal segregations of kerogen–bitumen (Hc) in association with pyrite (Py), pyrrhotite (Prt), and gold (Au); (b) close-up of panel (a): three gold (Au) grains at margins of kerogen–bitumen (Hc) segregations; (c) scattered kerogen–bitumen (Hc) ovoids in association with pyrite (Py) and chromite (Cr); (d) aggregative kerogen–bitumen (Hc) segregations and rims around quartz (Qz) in association with chromite (Cr), monazite (M), and pyrite (Py co).

Pr_2O_3, 0.38–4.64 Nd_2O_3, 0.03–0.70 Sm_2O_3, and 0.16–1.67 Gd_2O_3; 0.02–0.16 wt % UO_2 and 0.19–0.58 wt % ThO_2 were detected in some grains. Allanite was not described previously among minerals of ore-bearing reefs in the Witwatersrand Basin. Segregations of fine-grained titanite have been detected in the same mineral assemblage (Fig. 11d). In outer appearance, the amygdaloid basaltic andesite looks like an altered wall rock.

TYPOMORPHISM OF MAJOR MINERALS OF ORE-BEARING REEFS

In previous mineralogical studies, the main attention was paid to ore minerals, largely to pyrite, native gold, uraninite, and carbonic matter (kerogen–bitumen). Quartz was regarded as a rock-forming mineral, a product of diagenetic transformation of sediments and metamorphism of sedimentary rocks (Hallbauer, 1981; Volbrecht et al., 2002). In publications substantiating a model of hydrothermal metasomatic origin of gold mineralization in reefs (Phillips et al., 1989; Phillips and Myers, 1989; Law and Phillips, 2005), quartz was not studied in detail.

We focus our attention on the typomorphic features of quartz, pyrite, native gold, and their aggregates and assemblages, which provide insights into their formation conditions and mechanisms.

Pebble-shaped quartz is the major constituent of reefs. According to the adopted classification of sedimentary rocks (Kazansky et al., 1987), the "conglomerate" reefs should mostly be regarded as gravelly–pebbly rocks. "Rounded" lithic fragments in these rocks only occasionally are larger than 10 cm in diameter, while gravelly particles and fine- and medium-sized pebbles (1–5 mm) are the most abundant. Sporadic boulders up to 50 cm in diameter, which were found in the VCR, are composed largely of shale and sandstone. Quartz pebbles up to 20–25 cm in size are mentioned in

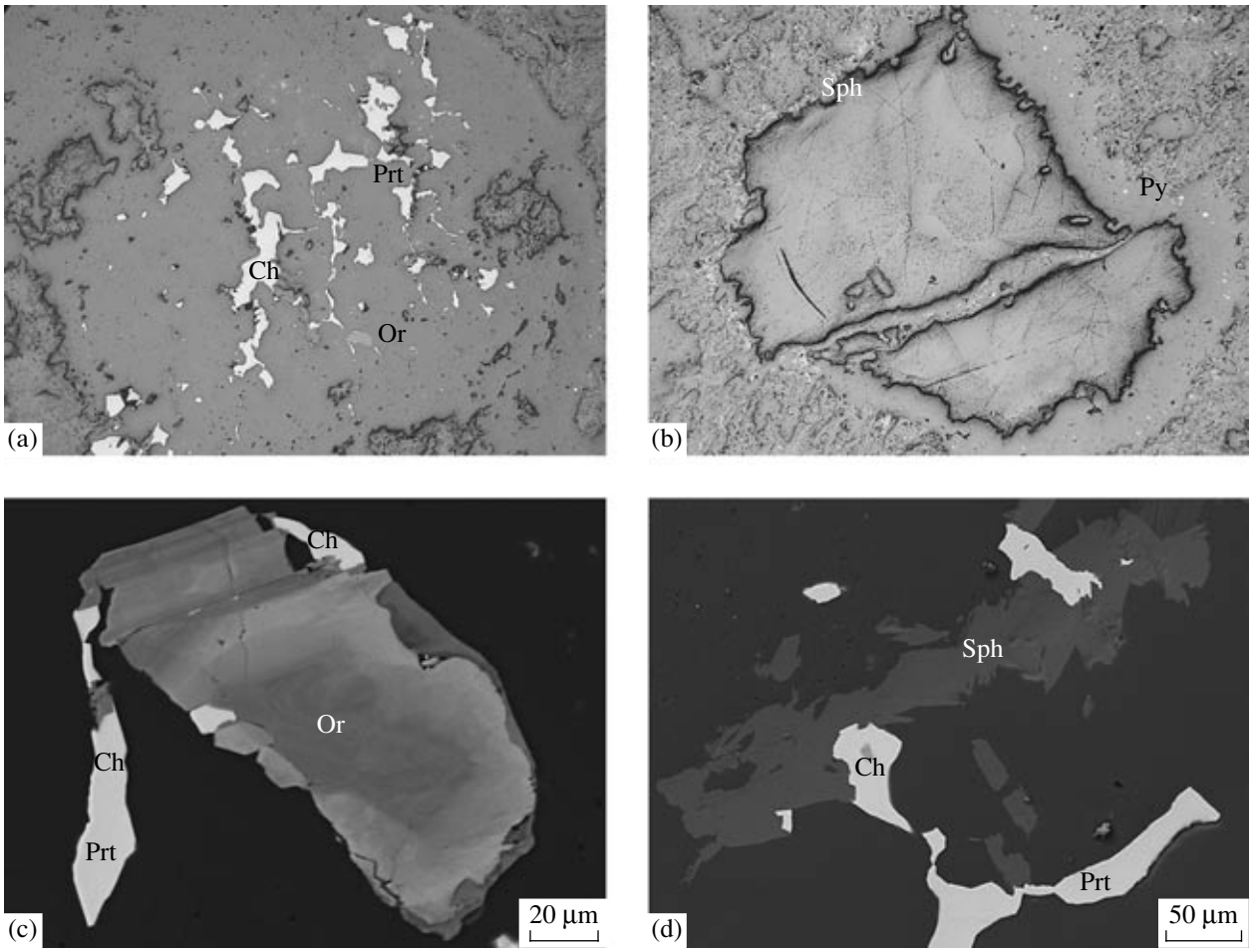

Fig. 11. Sulfide and REE mineralization in altered amygdaloid basaltic andesite. (a, b) Polished sections; horizontal width, 2.6 mm; (c, d) backscattered electron images obtained on a JEM-S300 electron microscope equipped with a Link ISIS energy dispersive X-ray spectrometer at the Institute of Geology of Ore Deposits, Petrography, Mineralogy, and Geochemistry, Russian Academy of Sciences, analyst A.V. Mokhov. (a) Pyrrhotite (Prt)–chalcopyrite (Ch) segregations in the quartz–chlorite fill of an amygdule; the gray grain is allanite; (b) chlorite fill of an amygdule; quartz with sphene (Sph) and pyrite (Py) disseminations; (c) zonal allanite in an intergrowth with chalcopyrite (Ch) and pyrrhotite (Prt).

the description of this reef as well. The proportions of quartz and lithic fragments in the gravelly–pebbly material of reefs vary in a narrow range: 70–90% is quartz, with the remainder comprising sandstones, shales, and sporadic volcanic rocks. Quartz is commonly considered to be a product of erosion of older veins. In a recent publication, Vollbrecht et al. (2002) applied optical and cathode luminescence microscopy to the study of quartz pebbles and cement from various ore-bearing reefs. A conclusion was drawn that most quartz grains were derived from felsic igneous rocks, whereas veined quartz in both pebbles and the psammitic fraction is virtually absent.

The variation in textural appearance of reefs expressed in the shape and sharpness of quartz pebbles and gravelly grains, as well as in the amount, dimensions, morphology, and spatial distribution of pyrite grains, was discussed above (Figs. 3, 5). Some quartz "pebbles" may be interpreted as products of crystallization of silica gel. Shcheglov (1994) reported examples of spherical "pebbles" up to "…pebbles of coarse-grained white quartz with shelly fine 'worms' of gold and pyrite in their core…."

Crystallization of ore-bearing silica gel and other transformations are considered by Kremenetsky et al. (1997, 2001) as a leading mechanism of "pebble" formation in ore-bearing reefs. This model is based on morphostructural analysis with the use of computer-aided optical geometric scanning of polished sections. The unimodal distribution of quartz "pebbles" in ore-bearing reefs is opposed to the bimodal distribution in the barren conglomerate units. The uniform composition of "pebbles" from the Black, Ventersdorp Contact, Carbon Leader, and other ore-bearing reefs, together with the uniform orientation of pebbles, is regarded as evidence for their autochthonous formation as silica gels (Kremenetsky et al., 1997, 2001).

The published photographs and the samples collected by us and looked through in collections of local geological surveys demonstrate that quartz is uniform in both the gravelly–pebbly fraction and the gravelly–sandy matrix in the Ventersdorp Contact, Carbon Leader, and other reefs. This statement relates mainly to the most abundant white and light gray quartz. Such quartz often composes "pebbles" of such a degree of roundness that they do not resemble clastic material even remotely. Quartz in such "pebbles" is often banded. Milky white, white, and light gray pebble-shaped quartz commonly occurs together with smoky, gray, and dark gray–black quartz. The latter is locally bleached in marginal zones and elsewhere. In the examined reefs, this quartz occurs largely as uniformly sized spherical "pebbles" 1.0–1.5 cm in diameter; larger pebbles of irregular morphology, occasionally elongated up to 10 cm, are extremely rare. Elevated LREE contents were established in dark gray quartz from Reef B (Welcom goldfield) and Cs was detected in a micrometer-sized grain of Ba orthoclase (Hallbauer and Kable, 1982; Hallbauer, 1983). As was established by the same authors, the opalescent quartz that often occurs in reefs and is described in several publications as opal or agate is distinguished by abundant microinclusions of calcite and apatite. The enrichment of pebble-shaped quartz in LREE was noted by Kremenetsky et al. (1997, 2001) as well. A positive correlation between La and Au in quartz with microinclusions of orthoclase, plagioclase, muscovite, chlorite, carbonates, apatite, corundum, and anhydrite, as well as pyrite, galena, chalcopyrite, and rutile, detected with electron microscopy was established by Hallbauer and Kable (1982).

The published geochemical data allow us to suggest a rare earth specialization of fluids responsible for crystallization of quartz in ore-bearing reefs. The revealed allanite mineralization supports this conclusion and emphasizes a common geochemical history of quartz belonging to different generations in ore-bearing reefs of the Witwatersrand Basin. In particular reefs, quartz exhibits specific assemblages of trace elements, which are discussed in the final section of this paper. Here, we only note the different modes of quartz occurrence in large mineral aggregates and in the groundmass. Chlorite–quartz nodules and pyrite–quartz "pebbles" composed of dark-colored very fine-grained quartz were described by Saager et al. (1982), Engelbrecht et al. (1986), and other authors. Chlorite–quartz fine-grained aggregates are typical of large pyrite nodules, described below. Medium-to-fine-grained quartz aggregates that correspond to psephitic and psammitic fractions are the most abundant in the reefs. Intergrowths of quartz grains of various dimensions, as well as veinlets, interstitial segregations, and sporadic micronodules of chlorite and sericite, are detected by microscopic examination. Chloritoid, which is observed as metacrysts in globular pyrite, is also detected in association with quartz and sericite. It is difficult to classify monocrystalline quartz grains and fine-grained aggregates (fragments) as primary or newly formed. The quartz grains that are equal to pyrite "pebbles" in size or smaller cover the entire morphological range of clastic fragments from angular to well-rounded. The latter are often located nearby larger quartz grains, irregular in outline but characterized by the same optical orientation, demonstrating disintegration of silica gel clots during colloidal mineral formation. One can judge the mechanism of quartz formation from relationships of this mineral with pyrite. Euhedral pyrite crystals associated with quartz indicate that this mineral completed its crystallization after pyrite (Fig. 12a). Roughly concentric segregations of pyrite around spherical quartz grains probably demonstrate coalescence of pyrite grains during formation of silica gel (Figs. 12b–12e). An effect of quartz "pebbles" on the symmetric arrangement of pyrite segregations and disseminations can be seen. Thereby, separate pyrite grains are close to the radius of a pebble in size.

Many specific morphological features of various generations of quartz and their relationships with other minerals observed in reefs may be explained by the colloidal–disperse state of a liquid phase that contained a greater or smaller amount of clastic material, the subsequent coagulation of colloids syneresis of gels, and the formation of residual true solutions.

The indicative relationships shown in Figs. 7–12 clearly demonstrate the granular texture of quartz. Figure 12e is especially noteworthy because the main fine-grained field of this figure is occupied by a shale fragment that is not replaced with either pyrite or quartz. It is suggestive that the largest grain of rounded porous or compact pyrite is separated from the shale by a thin quartz zone. A low reactivity of the fluid that formed the late pyrite with respect to the preceding generations of this mineral is illustrated by Figs. 13a–13d. The fine-grained quartz–pyrite aggregate with a small pyrite metacryst probably was retained as a relic of the early colloidal stage (Figs. 13d, 13e).

The rounded *pyrite* grains comprise compact allogenic detrital and concretionary globular and spherulitic varieties. The mechanisms of spherulite and concretion formation are rather clear; the same may be said about pyrite of mudball type. Rounded fragments of large pyrite concretions, as well as pyrite nodules and oolites with some amount of gangue minerals, have been described in a number of publications. Some of these nodules and oolites are composed of more than half gangue minerals, as, for example, a lenticular oolite from the Composite Reef that consists mainly of chlorite and pyrite (Tucker and Viljoen, 1986). A spherical agglomerate of compact pyrite, uraninite, chromite, chlorite, and pyrrhotite similar to those observed in the Carbon Leader and Vaal reefs is described in this publication. The authors point out that colloform nodular pyrite is abundant in the reef and a considerable amount of gold is related to this mineral. It is noted that pyrite was formed in an aqueous medium

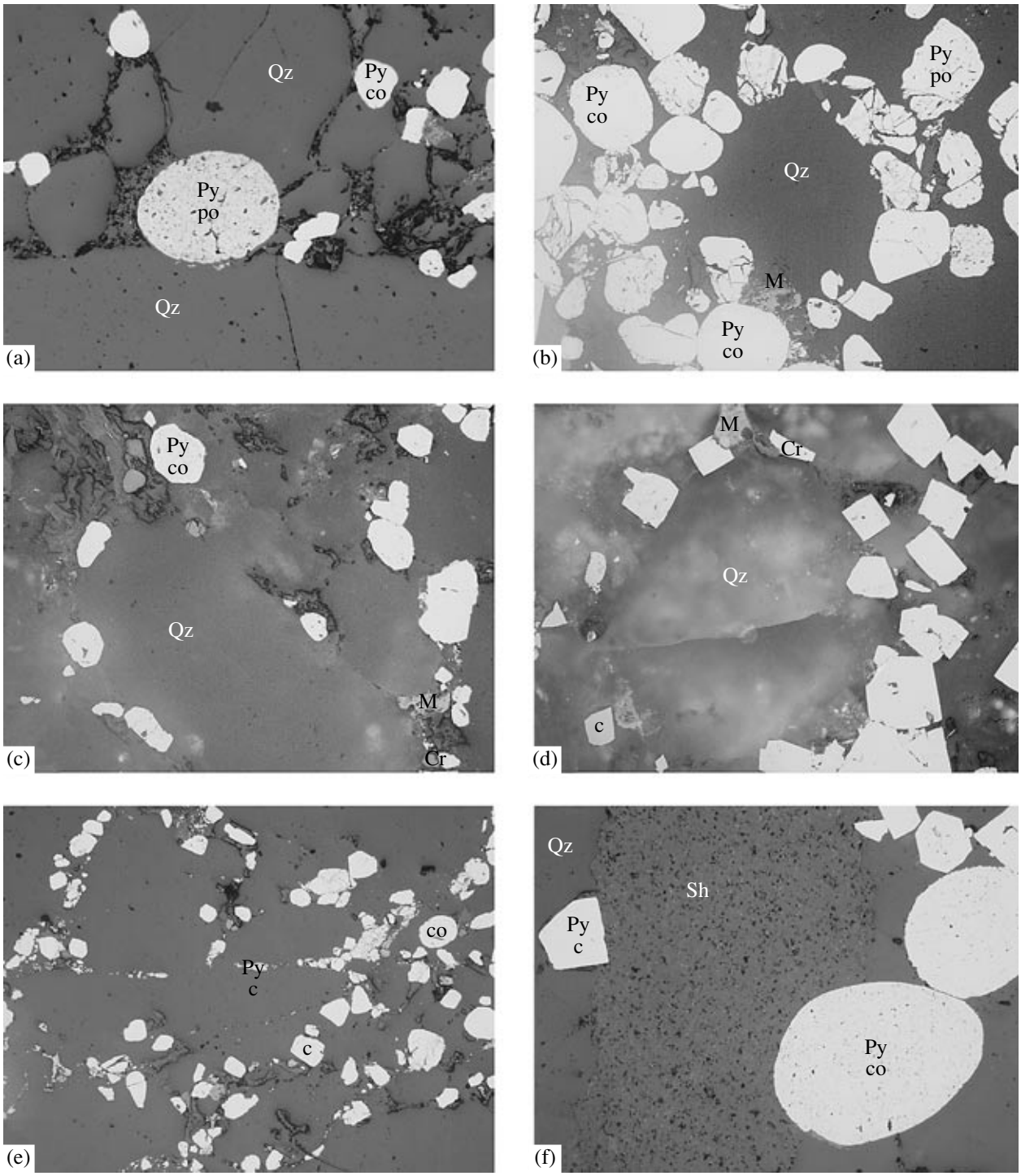

Fig. 12. Relationships between quartz and pyrite in the (a) Black, (b, c, e) Carbon Leader, and (d, f) Ventersdorp Contact reefs. Polished sections. Horizontal width (mm) (a–d) 1.3; (e) 2.6; (f) 1.3. (a) Euhedral grains of porous (po) and compact (co) pyrite in quartz (Qz); (b, c, e) compact (co) and crystalline (c) pyrites that rim pebble-shaped quartz; (d) crystalline (c) pyrite; (f) the main field is fine-grained altered shale (Sh); pyrites (po, c) in quartz (Qz); a quartz rim separates pyrite and shale.

and could have been transported for a short distance. The authors do not write about a colloidal origin of pyrite; however, such a possibility was often mentioned in previous publications. Fragments of large concretions and spherulites were observed only in the samples taken from the VCR. Spherulites with a clearly expressed marcasite texture (Fig. 14a), segregations of skeletal pyrite crystals and grains (Fig. 14b), and fragments of banded aggregates (Figs. 14c, 14d) are presented here. The reticulate texture of the pyrite–chlorite

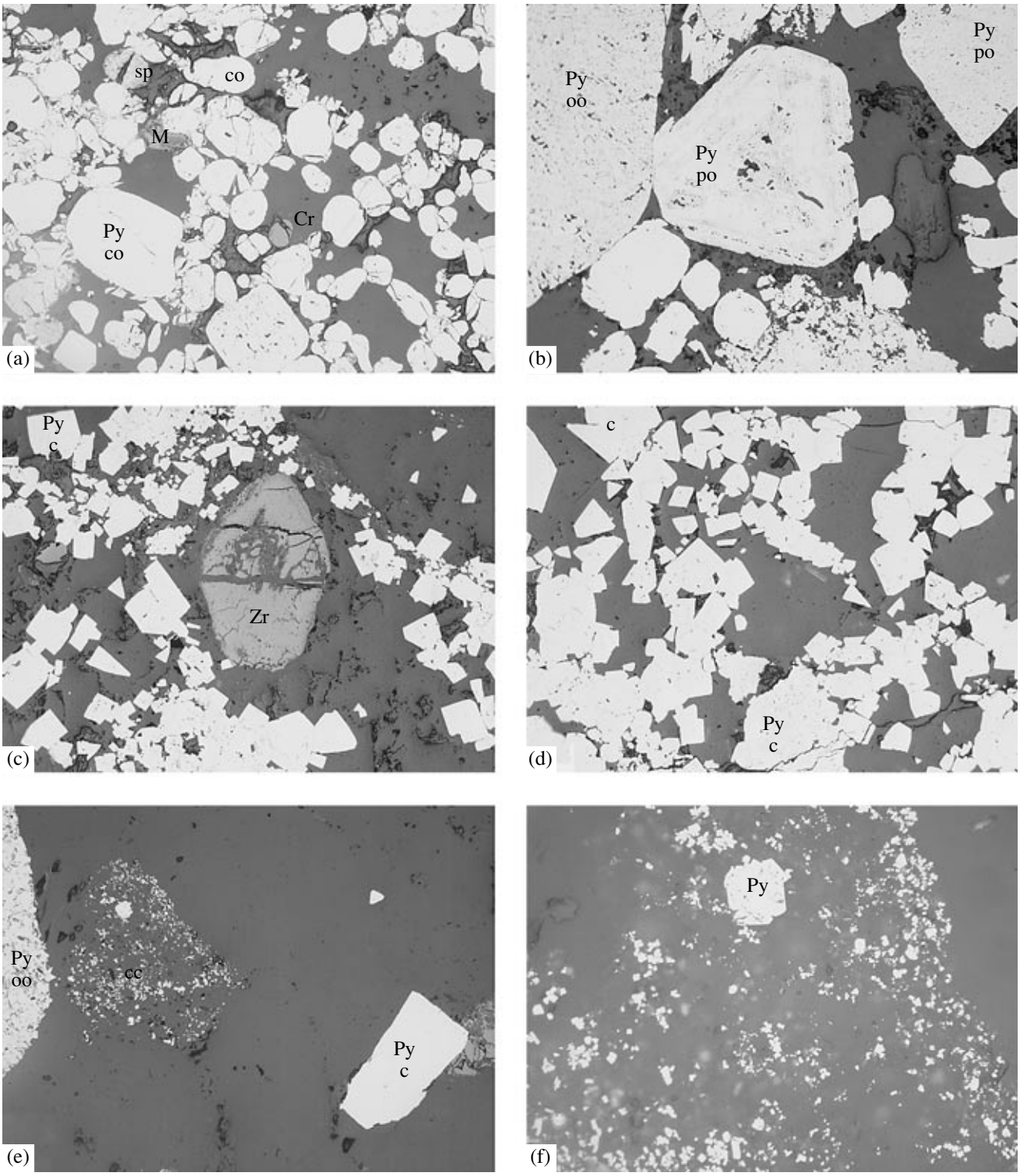

Fig. 13. Morphology of crystalline pyrite in the (a) Carbon Leader, (b, c, e, f) Ventersdorp Contact, and (d) Vaal reefs. Polished sections. Horizontal width (mm): (a, c, d) 2.6; (b, e) 1.3; (f) 0.65. (a) Medium- and fine-grained compact (co) and spherulitic (sp) pyrite, monazite (M), and chromite (Cr); (b) smoothed edges of a zonal pyrite crystal (co) and slightly corroded oolitic pyrite (Py oo); (c) crystalline (c) pyrite and corroded zircon (Zr) at the initial stage of disintegration; (d) crystals of pyrite (Py c) and their aggregates in quartz; (e) concretion of fine crystalline pyrite and oolitic (Py oo) pyrite; (f) close-up of panel (e), internal structure of a concretion with pyrite crystals (Py).

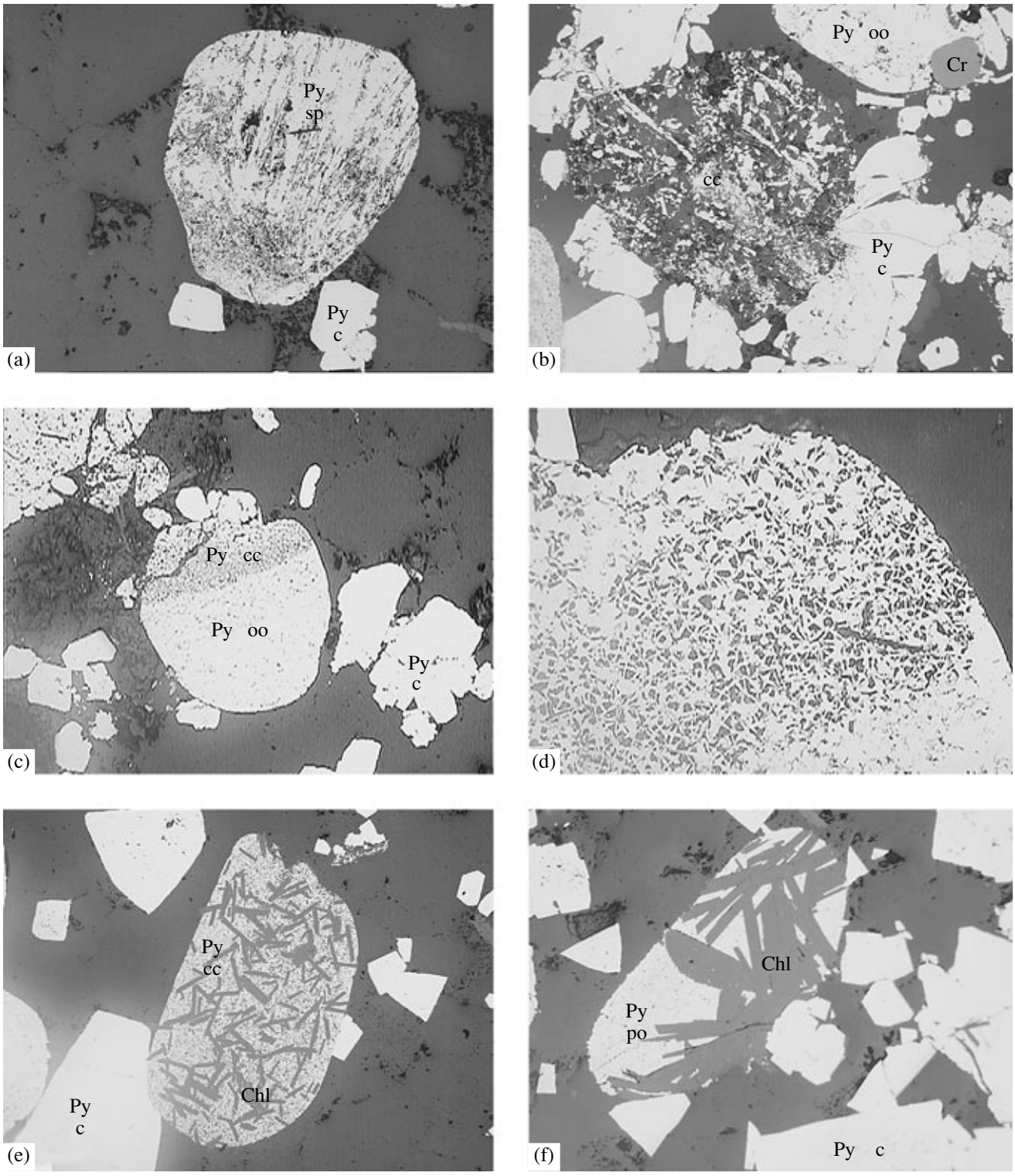

Fig. 14. Early spherulitic and nodular pyrites in the VCR. Polished sections. Horizontal width (mm): (a, b, c, f) 2.6; (e) 1.3; (d) 0.65. (a) Fragment of pyritic spherulite (Py sp) with marcasite structure and pyrite (Py c); (b) concretion of fine-grained and skeletal pyrite and oolitic (Py oo) pyrites, and chromite (Cr); (c) fragment of banded concretionary pyrite (Py cc) and oolitic pyrite (Py oo); (d) close-up of panel (c): the net structure of pyrite is visible; the interstices are filled with chlorite and quartz; (e, f) chloritoid (Chl) metacrysts in concretionary (cc) and porous (po) pyrite; quartz is dark gray.

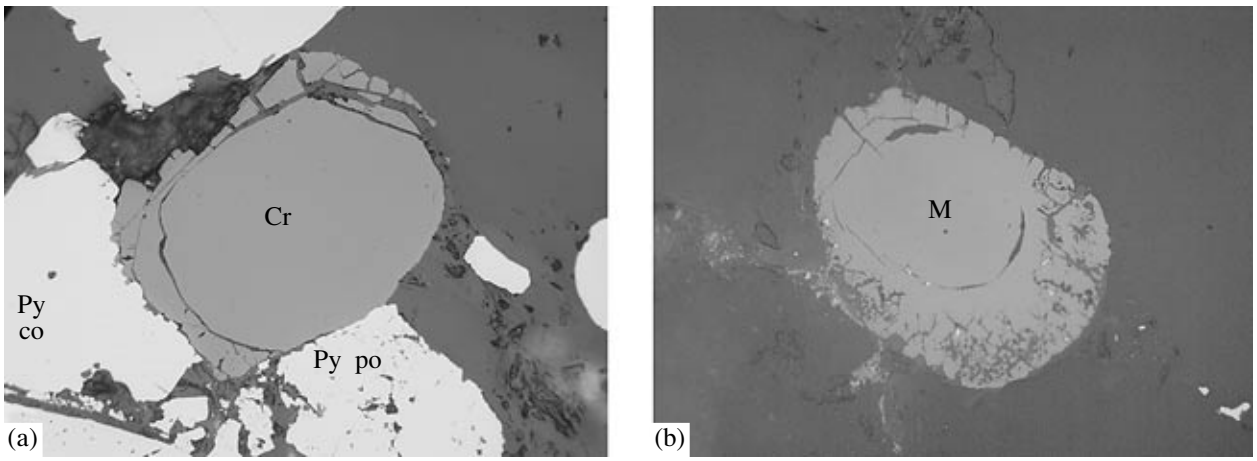

Fig. 15. Characteristic spherical fractures of initial disintegration in chromite and monazite. Polished sections; horizontal width, 0.65 mm. (a) Chromite (Cr) and pyrite (Py); the interstices in pyrite are filled with quartz, sericite, and potassium feldspar (VCR); (b) monazite with fine disseminations of ore minerals; quartz is dark gray (Vaal Reef).

zone in these aggregates is caused by the morphology of microscopic pyrite grains (Fig. 14d). Dispersed galena grains were detected in this zone with a microprobe. Oolites are commonly associated with porous and concretionary pyrite (Fig. 7) and occasionally contain chloritoid crystals (Figs. 14e, 14f). Selectivity in development of chloritoid metacrysts is noted rather frequently. The retention of the integrity of porous and globular pyrite along with development of chloritoid, as shown in Fig. 14f, unequivocally indicates that chloritoid is a newly formed, autochthonous mineral, whereas the fragments shown in Figs. 14a–14c are obviously allogenic. The concretionary and porous pyrites known from all reefs vary widely in degree of porosity and size of pores, from those similar to mudballs to those close to "compact" pyrite (Figs. 6–8). Mudball relics in compact (porous) pyrite (Fig. 8e) indicate that the latter mineral has a metasomatic origin in the Black Reef. At the same time, most concretions were probably formed as a result of segregation of uniform and nonuniform pyrite grains in a medium that contained various amounts of disperse suspensions.

The crystalline pyrite in reefs comprises younger (Figs. 13a, 13b) and older (Figs. 13c, 13d) generations. The rarely retained younger crystals mostly are pyritohedrons and octahedrons in habit. The stages when the normal growth of crystals ceased and they began to disintegrate are demonstrated in Figs. 13a and 13b. These stages were probably related to the passage of true solutions into colloidal solutions. The smoothing of edges of faces might be caused by corrosion, but no signs of this process were noted in the neighboring grains. The cessation of crystal growth apparently was one of two main mechanisms that led to the formation of rounded compact pyrites. The second and probably main mechanism of crystal rounding was, rather than rounding by mechanical grinding and abrasion, related to their hydrogenic (chemogenic) alteration, provoked by a change in the physicochemical state of the solution.

The fragments of arcuate, hemispheric fractures located in marginal zones of grains and oriented concordantly to the grain surfaces are important for understanding the formation mechanisms of rounded compact pyrites. In some cases, one can see torn-away surficial fragments of grains, including fragments faceted on one side and retaining arcuate outlines similar to the surface of rounded pyrite (Figs. 12b, 13a, 13b). The same rounding was observed in some chromite and monazite grains (Fig. 15). As can be seen from Fig. 15a, an appreciably corroded chromite grain became almost spherical owing to the propagation of a curvilinear fracture filled with quartz. Quartz–feldspar intergrowths were established here in pyrite with a microprobe. It is significant that the spherical fracture is closed up in chromite at the crystal face blocked by pyrite, while the torn-away chromite fragments are dismembered; some of them probably were dissolved (Fig. 15a). A central rounded core of a monazite grain is clearly seen as well (Fig. 15b). Recent publications have provided additional illustrations. Figure 4, I, from the paper by Frimmel et al. (2005) should be mentioned first of all. The initial and subsequent stages of the formation of spherical and other fractures in large crystals of compact pyrite are shown in this figure, as well as disintegration and corrosion of such crystals up to the separation of rounded grains.

A great body of the available information obtained with the microprobe concerns mineral inclusions in compact pyrites as both independent phases and minerals contained in fluid inclusions. This information was summarized in (Hallbauer and Kable, 1982; Hallbauer, 1983, 1986), including original data of these authors and a review of the results obtained by W. Hirders, C. Feather, R. Foster, S. Saager, T. Utter, and other researchers. The main objective of these studies was to

establish primary sources of detrital pyrite. However, the data obtained, including those regarding the trace element geochemistry of inclusions, provide additional insights into the origin of minerals that make up reefs as a common geochemical system. The list of minerals found as inclusions in compact pyrite comprises almost all species mentioned for pebble-shaped quartz and some other minerals as well; the former are the most frequent.

Quartz as inclusions in pyrite is the most abundant. The size of quartz inclusions varies from 1 to 20 μm. Chlorite and biotite are also common. Biotite contains an admixture of chrome. The data on fine gold, pyrite, and cobaltite inclusions in pyrophyllite are noteworthy. In addition to traditional Co, Ni, Cu, Pb, Zn, Ti, and As, Sn and occasionally Sc and La are noted as trace elements contained in pyrite. Au and Ag admixtures in pyrite are always detected in a wide range of contents (n–($n \times 10^2$) ppm). The Ag content is commonly lower than Au; however, compact pyrite is enriched in Ag relative to pyrites of other generations. Al, Mg, Ca, and Na are typical admixtures in compact pyrite ($n \times 1000$ ppm); K and Ba are contained in lesser concentrations ($n \times$ 100 ppm); Sr contents are still lower ($n \times 10$ ppm) but are elevated in some samples. The late pyrite crystals, mainly cubic in habit and smaller in size, were generally formed from solutions but in some cases replaced concretionary and compact pyrites.

Specific typomorphic features of *native gold* from the Witwatersrand Basin include the morphology and size of its grains and its composition, mineral assemblages, and abundance. Only toroidal gold as a product of eolian weathering may be reliably referred to as detrital grains (Minter, 1976). The main generations of gold may be classified as (i) associated with pebble-shaped quartz and early pyrite; (ii) associated with late sulfides, including pyrite, pyrrhotite, sphalerite, galena, and chalcopyrite; and (iii) associated with kerogen–bitumen segregations. The elevated Au content in pebble-shaped quartz and early pyrite, including rounded forms, is mainly related to finely dispersed native gold. Visible gold grains are rare. According to Hallbauer (1981), the average Au content in pyrite of this generation is about 10 ppm, in contrast to 1.5 ppm in the concretionary pyrite. An elevated Au content is typical of mudball-type pyrite (up to 600–900 ppm), although visible gold is extremely rare as well. It is suggested that the bottom mud was initially enriched in finely dispersed gold, which then was incorporated into pyrite as inclusions. Unfortunately, no data on the isomorphic admixture of gold in pyrite are available. The attributes of the detrital gold that experienced local alteration and transportation also remain unknown. The available information allows us to suggest that most gold is hydrothermal and related in its origin to the major mineral assemblages. The published descriptions of "detrital" grains intergrown with sphalerite, cobaltite–gersdorffite, bravoite, and sphalerite and chalcopyrite enriched in gold (from 250 to 6000 ppm, respectively), as well as pyrite–molybdenite intergrowths as "rounded" grains, may be regarded as evidence for complex evolution of mineral-forming systems in reefs and specific features of each reef, which are established from geochemical data, including variation in fineness of gold (800–1000, with a maximum at 850–950 units) and distribution of trace elements (Hg, Pt, Ir, Os, Re, Sb, Sn, Bi, Pb, Ag, Cd, Pd, Ru, Se, As, Ni, Co, Mn, Cr, V). Differences in composition of gold from various reefs are the most appreciable in concentrations of Ag, Hg, As, and other impurities.

Interesting data reported by Hallbauer (1986) concern the trace element contents in gold determined with INAA. In addition to Ag, Fe, Ni, Co, Zn, Sb, and Cu, the following elements (ppm) were detected in samples from four reefs: Sc (0.01–0.21), Zr (49–1200), Te (15–200), Ce (1.4–35.5), Eu (0.03–0.29), Yb (0.001), and Th (0.03–4.5; 284–427). The highest trace element contents were detected in gold from the Basal and B reefs in the Welcom goldfield. The assemblage of trace elements in gold is rather stable and comprises indicators of fluids related to mafic–ultramafic and granitic series.

Omitting the indicative characteristics of metalliferous kerogen–bitumen segregations, we note that they may be subdivided into three types: (i) containing significant amounts of pyrrhotite and chalcopyrite and less abundant sphalerite and galena; (ii) containing mainly uraninite, brannerite, and thucholite, as well as detrital (?) chromite, monazite, and compact pyrite; and (iii) carbonic proper. The Au content may be as high as 3%; 0.02–0.47% Ag, 0.02–0.12% Hg, 0.12–1.03% Th, and 1.88–7.28% U and Os, As, Sb, and Zn admixtures were established by Kable (1978) in 12 samples of carbonic matter from the Carbon Leader, Basal, and Vaal reefs (cited from Hallbauer, 1986). These samples obviously belong to the second type. The largest segregations of the third type (carbonic) that contain visible gold in high concentrations are regarded by many authors as biogenic in origin (Schidlovski, 1981; Hallbauer, 1981). The morphology of gold grains is attracted as an argument in favor of this interpretation. However, some attributes of gold are convergent and do not serve as direct evidence for a biogenic origin. For example, the same habits have been found in Au-bearing condensates of gases emitted in areas of active volcanism, i.e., at the Tolbachik volcano in Kamchatka (personal communication by I.V. Chaplygin).

FLUID INCLUSIONS IN QUARTZ

Fluid inclusions were studied in pebble-shaped quartz from the Black and Kimberley reefs (samples 17/02, 20/02 and 2/02, 3/02, respectively); quartz cement from the Ventersdorp Contact (sample 1/98), Black (sample 20/02), and Vaal (sample 55/98) reefs; and quartz from a vein in the footwall of the Kimberley Reef (samples 4/02, 5/02). The latter samples were taken from a trench that crosses this reef in the East Rand goldfield.

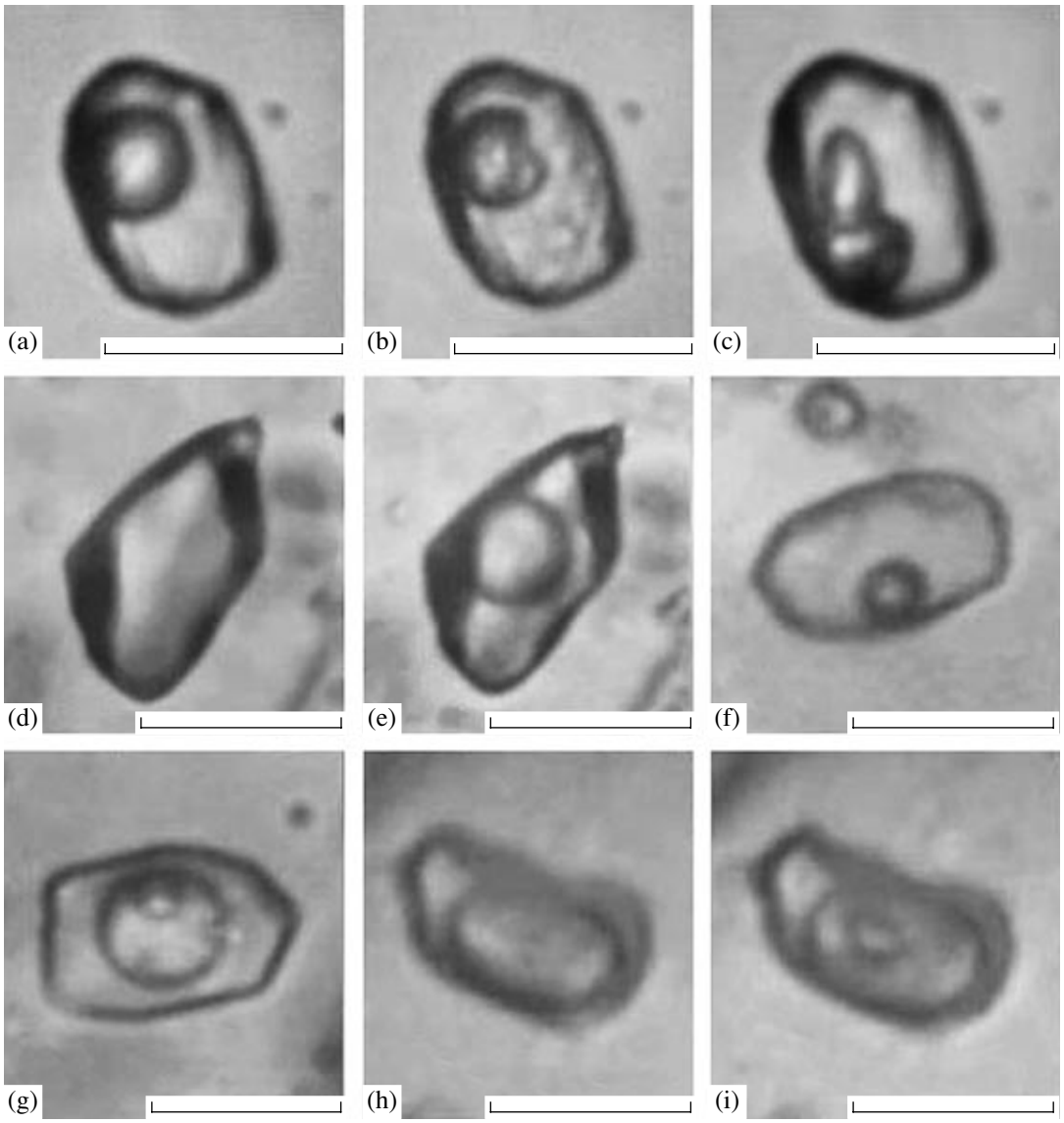

Fig. 16. Fluid inclusions in quartz. (a–f) Quartz from veins; (g–i) pebble-shaped quartz. (a–c) Inclusions of aqueous solution with a great amount of methane: (a) +20°C, (b) –95°C (liquid methane condenses in a gas bubble), (c) +5.9°C (gas hydrate grows); (d, e) substantially gaseous inclusions with dense hydrocarbons: (d) +20°C, (e) –55°C; (f) low-temperature fluid (gas + liquid) inclusion; (g) carbon dioxide–water fluid inclusion; (h, i) substantially gaseous inclusion with dense carbon dioxide: (h) +20°C and (i) +4.9°C. Scale bar is 10 μm.

Primary, pseudosecondary, and secondary fluid inclusions with various fills were found by the visual examination of transparent polished sheets 0.3–0.5 mm thick under a microscope at a great magnification (300–1200). As a rule, the size of the inclusions does not exceed 15 μm, and such a small size posed certain problems in their study. Two types of fluid inclusions were found in quartz from veins: (1) two-phase gas–liquid inclusions with a relatively large (22–30 vol %) gas bubble (Fig. 16a) and (2) substantially gaseous inclusions, dark at room temperature (Fig. 16d). Three types of fluid inclusions are present in pebble-shaped quartz: (3) carbon dioxide + water inclusions, with a gas bubble, liquid CO_2, and aqueous solution (Fig. 16g); (4) gaseous inclusions with liquid CO_2 and a rim of aqueous solution (Fig. 16h); and (5) two-phase gas–liquid inclusions with a small (3–10 vol %) gas bubble (Fig. 16f). All five types of fluid inclusions are observed in quartz from cement that is an aggregate of small, simultaneously crystallized grains. Fluid inclusions of types 1 and 2 were detected in one group of grains, and inclusions of types 3–5, in another group. There were no grains with all five types of inclusions.

The microthermometric studies were performed on a measuring complex designed at the Institute of Geology of Ore Deposits, Petrography, Mineralogy, and Geochemistry, Russian Academy of Sciences, on the basis of a THMSG-600 microscopic heating stage

Table 1. Composition of ore-forming fluids and physicochemical conditions of quartz formation in ore-bearing reefs of the Witwatersrand

Type of quartz	*n*	*T*, °C	*P*, bar	*C*, wt % NaCl equiv	CO_2/CH_4	$\frac{P^*_{total}}{P_{H_2O}}$	Notes
Vein	65	399–263	2030–160	8.6–4.8	0.16–0.04	7.5–1.0	Heterogeneous fluid; CH_4 and other hydrocarbons are predominant in the gas phase
Cement	78	294–145	1550–1450	18.1–2.6	n.a.	25.8–20.6	Two types of heterogeneous fluid; CO_2 prevails in the gas phase of one fluid and CH_4 and other hydrocarbons, in the gas phase of the other fluid
Pebble-shaped	98	314–149	1780–1470	13.5–2.4	2.45–1.19	45.9–15.3	Heterogeneous fluid with a prevalence of CO_2 in the gas phase

Note: *n* is the number of studied fluid inclusions; * index of the system's closedness; n.a., not analyzed.

(Linkam, England); an Amplival microscope (Germany) equipped with a set of long-focus objectives, including an Olympus 80× lens (Japan); a video camera; and a control computer. This complex makes possible on-line measurements of phase transition temperatures from –196 to +600°C, as well as digital photomicrography. The salt concentrations in fluid inclusions were estimated from temperatures of ice melting or dissolution of NaCl crystals (Bodnar and Vityk, 1994). The pressure of heterogeneous fluids was calculated from substantially gas-filled inclusions. The salt concentrations and fluid pressure were estimated with the FLINCOR program (Brown, 1989). The chemical composition of fluid inclusions in pebble-shaped and veined quartz was determined with various methods in charges 0.5 g in mass of the 0.50- to 0.25-mm fraction at the Central Institute of Geological Exploration for Base and Precious Metals (analyst Yu.V. Vasyuta) using methods described by Kryazhev et al. (2003). The amount of water necessary for calculation of element concentrations in fluid was determined preliminarily from the same charges.

Carbon dioxide, methane and other hydrocarbons, and chlorine were analyzed as well. After preparation of an extract, Na, Ca, and Mg, as well as a wide spectrum of ore and trace elements, were determined in solution with ICP MS; their concentrations were calculated relative to the water filling inclusions.

The results of the study of individual fluid inclusions are shown in Table 1 and Fig. 17, while the data

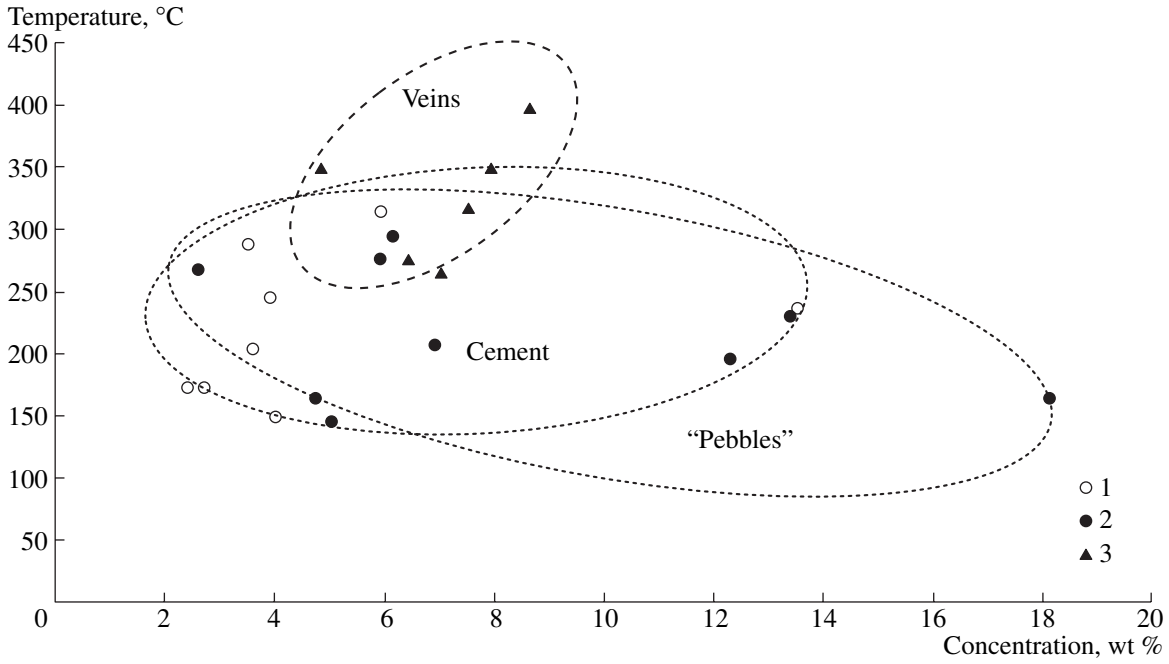

Fig. 17. Temperature versus concentration of mineral-forming fluids as deduced from the study of fluid inclusions in quartz from (1) cement, (2) pebbles in ore-bearing reefs, and (3) a barren vein.

Table 2. Concentrations of components in quartz from a vein in the Kimberley Reef and a "pebble" from the Vaal Reef (analyses of aqueous extracts from fluid inclusions)

Component, g/kg H_2O	Sample 4/02 (vein)	Sample 20/02 ("pebble")	Component, mg/kg H_2O	Sample 4/02 (vein)	Sample 20/02 ("pebble")
CO_2	10.14	2.41	Ge	0.58	0.92
CH_4	63.19	2.03	As	44.6	4.2
Saturated hydrocarbons	3.17	0.02	Br	333	137.7
Cl^-	34.39	17.93	Rb	2.3	1.1
SO_4^{2-}	3.97	–	Sr	279	127.13
HCO_3^-	18.02	19.09	Y	0.58	0.12
Na	15.86	12.82	Zr	3.0	0.4
Ca	12.62	4.89	Mo	0.7	0.12
Mg	0.41	0.25	Ag	0.29	–
Component, mg/kg H_2O			Cd	1.4	0.49
Li	1.5	3.8	Sb	8.7	0.43
B	21.8	9.1	Cs	17.7	2.8
Al	660	151.7	Ba	48	24.23
Sc	26.2	13.3	Hg	1.15	0.67
Cr	2.5	0.5	Tl	0.07	–
Mn	387	108.9	Pb	39.8	3.49
Co	2.3	–	Bi	0.07	–
Ni	33.6	–	Th	3.1	0.061
Cu	76	12.5	U	9.7	0.18
Ga	1.15	0.09	Mineralization, g/l	87	55

Note: Analyses were performed at the Central Institute of Geological Exploration for Base and Precious Metals, analyst Yu.V. Vasyuta.

on bulk samples are given in Table 2 and Fig. 18. The fluid inclusions of type 1 from quartz of veins contain an aqueous solution with a eutectic temperature varying from –36 to –23°C. This temperature testifies to the presence of dissolved Na and Mg (Borisenko, 1977). The salt concentration varies from 8.6 to 4.8 wt % NaCl equiv; the homogenization temperature is 349–263°C.

Liquid methane condenses in gas bubbles of some inclusions due to cooling (Fig. 16b), while gas hydrate grows due to thawing and disappears at a temperature above 14.0–14.8°C, also indicating the occurrence of methane. The methane concentration in solutions that fill fluid inclusions of this type amounts to 3.4 mol/kg of solution.

The syngenetic, substantially gaseous inclusions (type 2) contain dense (0.11–0.28 g/cm^3) methane (Fig. 16e). The study of the chemical composition (Table 2) confirmed that the fluid contains a great amount of methane; more complex saturated hydrocarbons were detected as well. The CO_2/CH_4 ratio varies from 0.04 to 0.16. The fluid pressure at 263–349°C was 160–2030 bars; the P_{tot}/P_{H_2O} ratio is 1.0–7.5 (Prokof'ev, 1998). The results of the fluid inclusion study in pebble-shaped quartz indicate a difference in the composition of the gas component. Fluid inclusions of type 3 contain carbon dioxide with a melting temperature of –(57.9–57.4)°C, which indicates a small admixture of low-boiling gases (the melting temperature of pure CO_2 is –56.6°C). The temperature of gas hydrate dissolution (7.8–11.2°C) supports the occurrence of methane (gas hydrates of CO_2 do not exist at temperatures above +10°C). The eutectic temperature of the solution is –(34–26)°C and thus indicates the presence of dissolved Na and Mg (Borisenko, 1977). The salt concentration is 3.5–6.2 wt % NaCl equiv; the homogenization temperature is 244–314°C. The CO_2 concentration in carbon dioxide–water fluid is 3.9–7.6 mol/kg of solution. The CO_2/CH_4 ratio varies from 1.2 to 2.5. Syngenetic inclusions of type 4 contain liquid CO_2 with a density of 0.78–0.85 g/cm^3 and with a small admixture of methane (the melting temperature is –(58.6–57.4)°C). The fluid pressure at 244–314°C attains 1470–1780 bars. The P_{tot}/P_{H_2O} ratio is 15.3–45.9. Fluid inclusions of type 5 are homogenized into liquid at 149–236°C and contain an aqueous solution of Mg and Na chlorides (the eutectic temperature is –(43–25)°C) with a salt

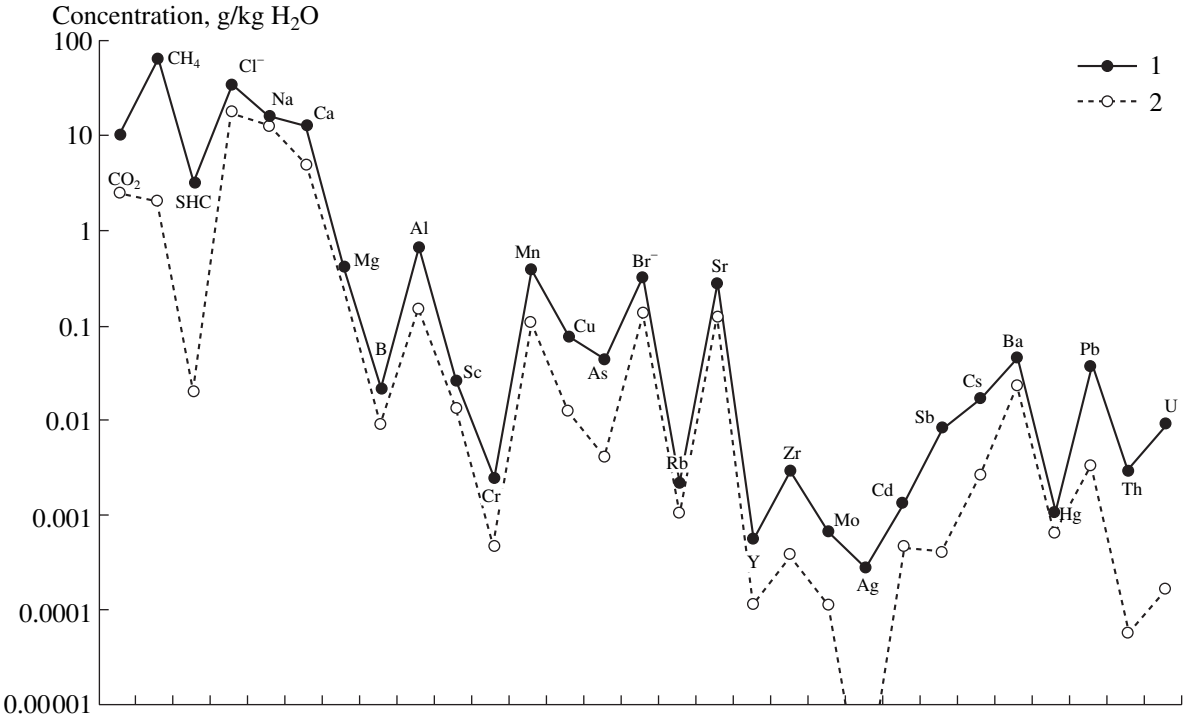

Fig. 18. Concentrations of chemical elements in solutions from fluid inclusions in (1) veins and (2) quartz "pebbles": analyses of aqueous extracts with gas and ion chromatography and ICP MS. SHC are saturated hydrocarbons.

concentration of 2.4–13.5 wt % NaCl equiv. The bulk chemical composition confirmed the occurrence of CO_2, Cl, Mg, and Na in solutions that fill inclusions.

All types of inclusions and all transitional compositions of fluids were revealed in quartz of cement. The temperature of their capture is 145–294°C, the pressure is 1450–1550 bars, the salt concentration is 2.6–18.1 wt % NaCl equiv, and the P_{tot}/P_{H_2O} ratio is 20.6–25.8.

The results obtained indicate that the parameters of formation of quartz "pebbles" and cement are close to one another (Tables 1, 2; Fig. 17), though they vary in a wide range. This may be partly caused by a limited number of study objects; however, in any case, this similarity should be kept in mind while the formation conditions of reefs are interpreted. It should be noted that the physicochemical conditions of quartz vein formation are characterized by a wider range of pressures and a lesser degree of closedness of a system, indicating a difference in processes responsible for formation of "conglomerates" and quartz veins. At the same time, the common chemical composition of fluid inclusions (Fig. 18) in quartz from veins and "pebbles" in the Black Reef may be attributed to the common geochemical specialization of deep sources of fluids. The close physicochemical parameters of fluids captured by quartz of "pebbles" and cement may testify in favor of their conjugate formation. The revealed differences in chemical compositions of fluid inclusions in quartz from "pebbles" and cement may be accounted for by a drastic change in redox conditions of the mineral-forming medium in the course of formation or recrystallization of Au-bearing conglomerates. Such gradients indicate a high viscosity and poor permeability of the medium during quartz formation due to the gel-like state of silica in the process of reef development. The gradients of redox conditions might affect the mineral formation in reefs.

A GENETIC MODEL OF ORE-BEARING REEFS IN THE WITWATERSRAND BASIN

The model of synsedimentation hydrothermal formation of ore-bearing reefs in the Witwatersrand Basin undoubtedly requires further substantiation and development taking into account the complex combination of unique processes of exo- and endogenic mineral formation. The acceptance of a nondetrital origin of pebble-shaped quartz is crucial in this respect. The formation of rounded pyrite grains by hydrogenic (chemogenic) alteration of crystals or their aggregates during partial (regulated) crystallization in semicolloidal and colloidal solutions, as well as by replacement and recrystallization of older pyrites, is not an anomalous phenomenon. These mechanisms are consistent with general laws of colloidal mineral formation in various geological media (Chukhrov, 1955; Betekhtin et al., 1958; Lebedev, 1965; Kigai, 1974) and are exhibited at various deposits.

Hutchinson and Viljoen (1988) pointed out the rounded pyrite at the Agnico-Eagle massive sulfide

deposit. Such pyrites are known from the massive sulfide deposits of the Rudny Altai. High-temperature quartz and pyrite globules from a few millimeters to 2–5 cm in diameter were retained here after the metamorphism of ore (Popov et al., 1995).

Borodaevskaya and Krivtsov (1970) suggested that, at massive sulfide deposits, not only sulfides in orebodies but also quartz–sulfide aggregates in metasomatically altered wall rocks are metacolloidal in origin. These authors emphasized the great importance of studying "gel metasomatism" (Lindgren, 1925). Pyrite "oolites" at the Kvartsitovy Gorki (Quartzite Hills) gold deposit in northern Kazakhstan were formed as products of metasomatism at a medium depth. The morphological and structural similarity of rounded pyrites and the common mechanism of their formation in the reefs of the Witwatersrand Basin and at the Kochbulak deposit were shown previously (Safonov, 2003, 2004). Let us illustrate some of these mechanisms. Figure 19a demonstrates a rounded pyrite grain that was formed by disintegration of the outer zone of a large pyrite metacryst with a relic of older porous metacolloidal pyrite; the stages of preliminary and complete disintegration that predated dispersion and dissolution of fragments are shown in Figs. 19b and 19c, respectively. The cessation of normal growth of pyrite, its transformation into a hemisphere, and the coalescence of small pyrite grains are displayed in Fig. 19d. Finally, closeups of colloform pyrite–quartz aggregates display the consequences of the early crystallization of silica gel with the formation of very fine-grained Au-bearing quartz–pyrite cement (Fig. 19e). The later aggregates of angular and rounded grains of compact pyrite were formed from new colloidal solutions (Fig. 19f). The textural similarity of these images and some segments of the Witwatersrand reefs, as well as photomicrographs of chromite and monazite (Fig. 15) and pyrite (presented by Frimmel et al. (2005)), indicate that the suggested mechanisms of rounded pyrite formation are realistic. Rare relict colloidal textures retained in "pebbles" of irregular shape and the similarity of quartz from such pebbles over large segments of reefs, often accompanied by homogeneous gravelly material, serve as direct evidence for the metacolloidal origin of a significant part of pebbles and gravel in ore-bearing reefs. Quartz "pebbles" with clearly expressed effects of opalescence may be regarded as indicators of primary colloidal mineral formation. These "pebbles" correspond to the lower size level of the pebbles and clastic material of reefs. The gravel fraction (<5 mm) is the most abundant and contains lithic fragments; according to Vollbrecht et al. (2002), this fraction is devoid of quartz vein fragments. We do not know what reference collections were used by these researchers, and, therefore, their conclusions cannot be accepted as unequivocal. The specific texture of metacolloidal quartz is retained locally in the gravel fraction. The primary colloidal state of solutions in sedimentary rocks might explain the surprisingly wide range of thicknesses of Au-bearing reefs, from 1 cm to 10 m, as well as the scattering of thin interlayers; their lenticular, disklike morphology; and the rather large globular segregations of Au- and sulfide-bearing quartz in shales. These phenomena are especially characteristic of the Basal Reef and VCR. High-density colloidal solutions can transport detrital heavy minerals. As has been shown by many authors, the distribution of these minerals in the reefs does not obey the laws of gravitational and hydrodynamic differentiation typical of placer and clastic rock formation in the normal sedimentation cycle.

According to Vollbrecht et al. (2002), the main stages of formation of reefs as geological bodies comprise sedimentation; diagenesis; and pre-, syn-, and postmetamorphic transformation of rocks. The stages of cata- and metagenesis of terrigenous rocks, accepted in the Russian literature (Yapaskurt, 2005), are omitted in this scheme. The main process of lithification of sediments is related to diagenesis and is reinforced during metamorphism. The real mechanisms of these processes in the course of formation of intracontinental basins have been studied insufficiently, and the interpretation of hydrothermal–sedimentary processes in the Witwatersrand Basin meets with problems in this respect. Nevertheless, the information gathered allows us to consider some key issues concerning the history of ore-bearing reef formation. In addition to general indications of the early lithification of sediments at the stage of diagenesis (Vollbrecht et al., 2002), the occurrence of xenoliths of the mineralized reef in the overlying basalts and basaltic extrusions (tectonic sheets?) within the reef is important evidence that constrains the time of consolidation of the Ventersdorp Reef. As was shown above, the contact zone of amygdaloid basaltic andesite experienced chlorite–quartz alteration and bears sulfide assemblage associated with REE mineralization like that of the ore-bearing reef itself. Whiteside (1981) reported that a borehole drilled in the western part of the West Deep Levels crossed basalts with visible gold at a distance of 15 cm from the contact with the VCR. Thus, it may be suggested that the late sulfide mineralization in reefs developed synchronously with mineral filling of amygdules in the contact zone of basalts, while the completion of lithification of reefs may be synchronized with the onset of volcanic eruptions. The minimal temperature of epigenetic quartz formation in reefs was established at 110–150°C by Hallbauer and Kable (1982) and confirmed by our investigations. This temperature is quite suitable for crystallization and structurization of silica gel. The arising mineral system becomes partly closed, and the pressure therein can be higher than the lithostatic level. The *PT* parameters of such a system are lower than those typical of metamorphism. Having studied fluid inclusions in quartz cement, Vollbrecht et al. (2002) estimated

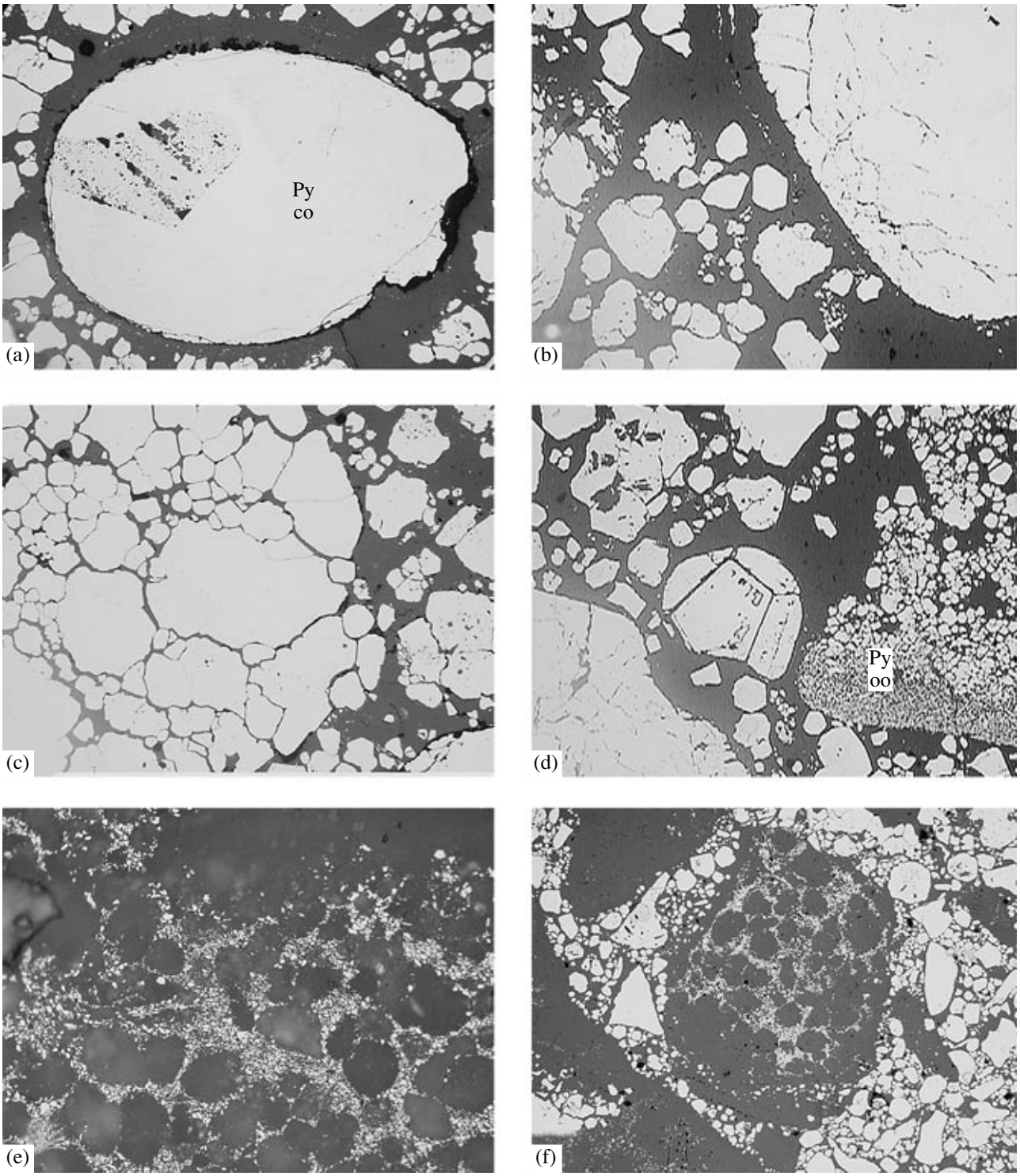

Fig. 19. Mechanisms of rounded pyrite formation at the Kochbulak deposit. Polished sections. Horizontal width (mm): (a–d) 2.6; (e) 0.65; (f) 1.3. (a) Rounded pyrite crystal (Py co) with corroded and disintegrated outer zone; (b) "hydrogenic" microfractures in a large pyrite crystal; fine relics of pyrite are seen in the surrounding quartz mass; (c) main stage of disintegration of the rounded grain of compact pyrite; (d) cessation of growth of a pyrite crystal and its transformation into a hemisphere (in center) contemporaneously with formation of pyritic oolites (Py oo); (e) quartz nodules cemented by a fine-grained quartz–pyrite mass; on the left, a residual geode; (f) fragments of colloform pyrite–quartz aggregate within crystallized metacolloids with rounded and "clastic" pyrite.

the *PT* interval of cement formation at 180 bar/90°C–760 bar/205°C. According to Frimmel et al. (1993), the temperature of quartz cement formation in the Basal Reef was 130–140°C, whereas the general *PT* parameters of metamorphism are accepted, following Phillips (1987), as 2.5–3.0 kbar and 350 ± 50°C on the basis of

thermobarometric results and mineral (chlorite, pyrophyllite) geothermometers (Frimmel et al., 2005).

In general, the available data on *PT* conditions of mineral formation in reefs have remained insufficient for estimation of the evolution of ore-forming systems related to specific reefs located at different depths.

The level of study of physicochemical conditions of ore formation, including transformation of particular minerals and their assemblages, may be assessed in the same way. This problem has been discussed for a long time. In terms of the model of modified paleoplacers, a reducing or slightly oxidizing regime of the aqueous environment is accepted in accordance with the state of the atmosphere, reduced and saturated with hydrogen sulfide, in the opinion of some authors, or containing a small amount of oxygen, as suggested by England et al. (2002) and Frimmel et al. (2005). These estimates are based on detrital assemblages of heavy minerals and the morphological appearance of these minerals. As was shown above, such criteria are insufficient for estimation of the state of the environment. The data on reactive surface waters with temperatures close to 100°C are more convincing. However, the general information on the Archean and Paleoproterozoic atmosphere and hydrosphere does not allow us to estimate, even approximately, the possible composition of water in the basin and thus to constrain the corresponding gain of components by reefs. The general polyelemental geochemical specialization of ore-forming fluids deduced from trace elements in fluid inclusions and mineral assemblages (Si, Au, Fe, Cu, Zn, Pb, Ni, Co, Cr, Ti, U, Th, REE, Os, Ir) cannot be accepted as identical to the primary specialization of the sedimentary basin. The speciation of these elements in fluids is ensured by compounds containing K; Na; and, especially, S, C, and Cl. The data obtained suggest that the formation of ore-bearing reefs was related to supply of endogenic fluids into the marginal parts of the basin and their mixing with near-surface water, which was particularly active in channeled flows. Most important in this respect are gas-saturated fluids that transport H_2S, CO_2, and CH_4; volatile compounds of ore elements; and hydrocarbons.

The sulfur isotopic composition of pyrite indicates heterogeneity of ore-forming fluids. The "detrital" pyrites are characterized by a wide range of $\delta^{34}S$ (from –7 to +32‰) and the authigenic crystalline pyrite, by a narrow range (from –0.5 to +2.5‰) (Frimmel et al., 2005). Kremenetsky and Yushko (1990); Kremenetsky et al. (2001) established a narrower scatter and showed that positive $\delta^{34}S$ values are characteristic of compact and partly of crystalline pyrites, including those partly replaced with other sulfides (pyrrhotite, chalcopyrite, etc.), whereas negative values of (–3.8–3.9‰) are typical of porous and oolitic rounded pyrites. Taking into account that pyrite studied with laser ablation (England et al., 2002) revealed a wide variation in $\delta^{34}S$ (from –4.7 to +6.7‰) in neighboring grains and even within one grain, the assumption that pyrite grains were affected by mixed solutions along with retention of hydrogen sulfide in the gas phase of fluids receives additional support.

The role of hydrocarbons in the transport of ore components remains unclear. Along with the concept of a biogenic origin of the kerogen–bitumen matter in ore-bearing reefs (Armstrong, 1981), the information gained testifies to the primary, endogenic nature of hydrocarbons (Maksimyuk and Kremenetsky, 2001). Our investigations with participation of specialists in different fields revealed both exogenic (biogenic) compounds and compounds identical to those detected in mantle xenoliths. The carbon isotopic composition also indicates an endogenic source of most carbonic substances and their appreciable transformation at various depths during diagenesis and metamorphism (Safonov et al., 2000, 2001). The morphology of segregations of carbonic matter and their distribution in reefs show that some of these segregations were not modified in the process of lithification, probably, due to their retention in voids of crystalline material.

The morphology of segregations of organic matter in ore-bearing reefs, including the aforementioned carbonic laminae, may be explained in terms of their metacolloidal formation and precipitation from residual solutions. The close relations of uraninite and brannerite to carbonic matter and brannerite inclusions in pyrite do not allow us to regard these minerals as allogenic. Their shape probably was controlled by the same mechanisms of crystal rounding that were discussed above, as well as by partial replacement by hydrocarbons. The reactivity of the late hydrothermal solutions is reflected in replacement of outer zones of pyrite and chromite grains with hydrocarbons.

The distribution of Cr as an admixture in ore and gangue minerals contained in reefs and the occurrence of fuchsite and Cr-bearing sericite admit an endogenic origin of chromite. The data on Zn-bearing chromite (Hallbauer, 1983; Barton and Hallbauer, 1996) similar to that known from massive sulfide deposits attract attention.

The model of synsedimentation hydrothermal formation of reefs, like the model of metasomatic replacement, is inconsistent with determinations of isotopic age, especially with recent results. It was supposed that paleoplacers were formed 2.9–2.7 Ga ago in the Witwatersrand Basin and ~2.5 Ga ago in the Black Reef. Nevertheless, the age of uranium mineralization remains uncertain and embraces the interval from 2.5 to 1.0 Ga. These data, obtained from U/Pb isotope ratios, and the conclusions drawn by Barton and Hallbauer (1996) on an Archean age (~3 Ga) of allogenic pyrites in the Black Reef, against an age of 2.5 Ga for authigenic pyrites, testify to complex chronological relationships in sources of endogenic fluids and in the formation of minerals-carriers. The same may be said about Re–Os estimates of pyrite and gold ages (Kirk et al., 2001; Frimmel et al., 2005), especially as osmium is a com-

ponent of productive mineralization. The authors of the metasomatic model of reef formation connect this process with endogenic activity that occurred 2 Ga ago and explain the discordant ages by methodological problems of isotope geochronology (Law and Phillips, 2005). The Re–Os age of ~3 Ga, as well as the same age of compact pyrite in the Vaal Reef, are of genetic importance; however, in outward appearance, these estimates may serve as direct evidence for a detrital origin of these minerals because, according to new data (Frimmel et al., 2005), the age of the Central Rand Group is 2.90–2.84 Ga. Thus, the compact pyrite and gold in the Vaal Reef were formed at the same time and probably from the same fluid.

In general, the proposed model may be regarded as a variant of sedimentary–exhalation (sedex) or hydrothermal–sedimentary concepts. Defining the reef formation as synsedimentation, we emphasize not only its synchronism with sedimentation but also the active circulation of formational and pore water in the already formed sediments. The ore-forming process proper is regarded as a hydrothermal one. The standard mechanisms of deposition of terrigenous material were limited or completely suppressed. The specific character of the formation of ore-bearing reefs in the Witwatersrand Basin is primarily related to the behavior of silica as the major component of ore-forming systems. The particular systems that corresponded to the major reefs probably were formed as a result of a single episode of component supply and developed as closed or partly closed systems. Such evolution may be characterized as self-development that is completed with the deposition of the main mass of gold. The formation of uranium and carbonic mineralization is not considered here. It should only be noted that the adherents of the metasomatic hydrothermal model and the researchers who assume the substantial metamorphism of paleoplacers accept the following sequence of involvement of major elements in the active hydrothermal process: U–C–Au (Phillips and Myers, 1989; Law and Phillips, 2005; Frimmel et al., 2005). According to our model, the sequence is reverse.

A flow sheet of the evolution of a particular synsedimentation hydrothermal system is shown in Fig. 20.

The following stages are recognized in the formation history of the major reefs: (i) formation of a colloidal–disperse Au-bearing system, (ii) development of this system and its transformation into a dynamic mineral system, and (iii) consolidation and alteration of the mineral system. The initial, roughly disperse state of the system was controlled by sedimentation, where varisized mineral particles and lithic fragments were suspended in water and sediments of various settings (channels, terraces, etc.). The colloidal–disperse system originated under the effect of an external fluid impact. At the first stage of the colloidal system evolution, the disperse phase comprised silica and pyrite particles, aerosols, and macro- and microparticles of rock- and ore-forming minerals. The larger lithic fragments, including gravel and pebbles, served as an environment that exerted a certain influence upon the development of the ore-forming colloidal–disperse system proper. The quantitative proportions of the terrigenous material and fluids, including disperse phases, varied in a wide range from one reef to another. They were also variable within particular reefs. The VCR is distinguished by the most complex evolution (Vermaakt and Chunett, 1994). The water flows acquired a colloidal state immediately after mixing with endogenic fluids. The spread of colloidal solutions depended on the general hydrodynamic conditions, the mass of the gained fluids, and the duration of their supply. The morphology and internal structure of large reefs allow the suggestion of a stationary regime of gas-saturated fluid supply and mixing of this fluid with both surface and formational waters. A part of sedimentary material was probably dissolved, and heterogeneous particles experienced gravitational differentiation. Marcasite and the early generation of pyrite, conditionally called exhalation minerals due to their similarity to the same minerals at massive sulfide deposits, were formed during supply of endogenic fluids. Afterward, they were destroyed and dispersed in a flow of solution. The transition of the colloidal–disperse system into a gel and coagulation of colloids started after a certain saturation of the solution and formation of clots composed of silica gel I and comparable in size with lithic pebbles. Spherulites and segregations of iron sulfides were formed at the same time. During formation and partial crystallization of gels, the dispersion medium passed into a semicolloidal state or into true solutions, from which the compact pyrite I crystallized. The main mass of pyrite in reefs, as well as arsenopyrite and Ni and Co sulfides, was formed during crystallization of silica gel I, probably, due to the loss of H_2S dissolved in solution. As is known, hydrogen sulfide exerts a protective effect on silica colloids (Chukhrov, 1955).

Silica gel of the second stage probably formed gradually with transition of true solutions into semicolloidal and colloidal states. This process might be a consequence of a compositional change in the dispersion medium related not only to the loss of H_2S but also to capture of trace elements, gold, and other components by silica gel I and ore minerals. The authigenic pyrite nodules and segregations, as well as porous pyrite, were formed at that time, largely at the expense of fragments of the rounded compact and exhalation pyrite.

The dimensions of quartz and pyrite segregations of various generations were probably determined by effects of alluvial gravel, pebbles, and sand on the structure of electrochemical bonds in the dispersion medium. The destruction of mineral aggregates and grains and their rounding obeyed parameters of crystallochemical symmetry during crystallization of minerals different in density and electrochemical characteristics, as follows from the crystal chemistry of natural minerals and colloidal systems. Gold was deposited together

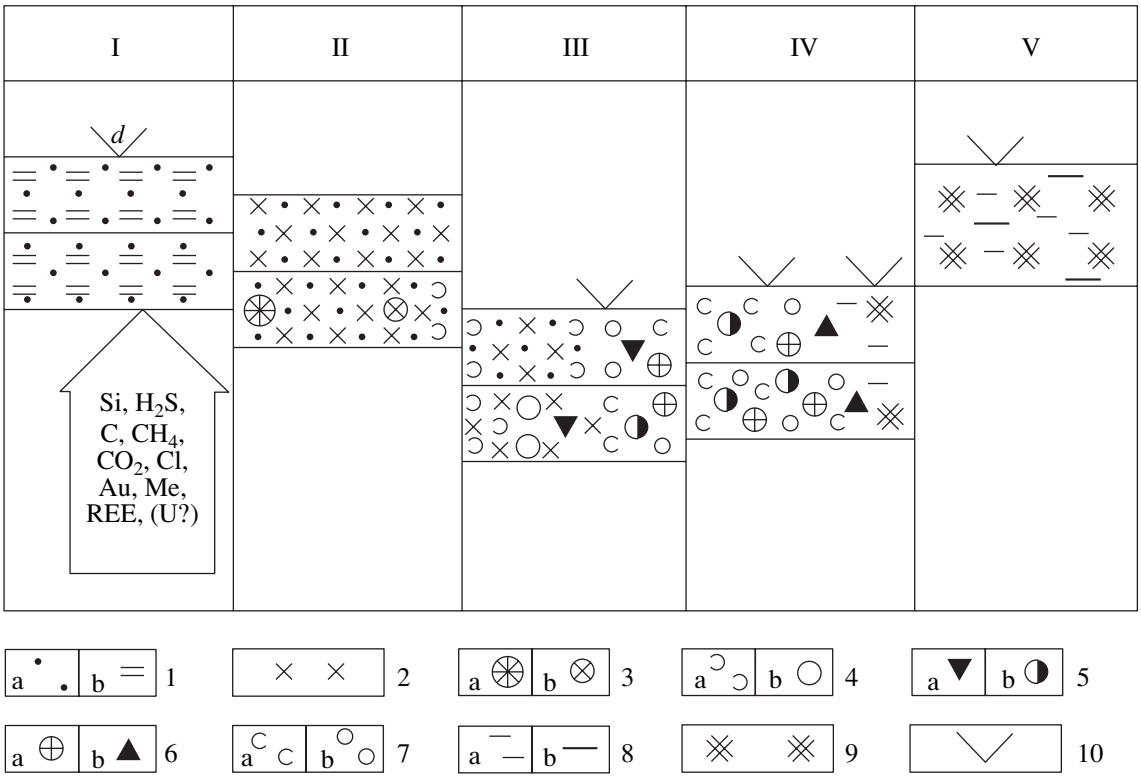

Fig. 20. Model of origin and evolution of a particular synsedimentation ore-forming system. (I) Disperse aqueous system; (II–IV) ore-bearing colloidal–disperse system: (II) initial stage, (III) stage of formation and crystallization of silica gel I, (IV) stage of formation of silica gel II and coacervation of pyrite grains; transitions between stages are gradual; (V) mineral system. (1) Aqueous medium with (a) suspended particles and (b) primary sediments; (2) colloidal dispersion medium; (3a) "exhalation" pyrite and (3b) its displaced fragments; (4a) silica gel I and (4b) pebble-shaped nodular quartz; (5a) compact crystalline pyrite and (5b) its rounded fragments; (6a) concretionary, porous, and newly formed spherulitic pyrites and (6b) crystalline pyrite of the late generation; (7a) silica gel II and (7b) crystallized "gravelly–sandy" quartz; (8) formation of (a) late sulfide and (b) kerogen–bitumen assemblages; (9) mineral system; (10) gold deposition (*d* is detrital gold). The chronological variation in depth of the system is shown.

with compact pyrite and later on, during crystallization of silica gel II, which completed the formation of the frameworks of reefs as mineral bodies. The mineral formation in these bodies proceeded further. Minerals of the late sulfide assemblage—pyrrhotite, chalcopyrite, sphalerite, and less abundant galena—precipitated from residual solutions along with carbonic matter, gold, and uranium minerals. The localization of especially this mineral assemblage is controlled by tectonic factors, which are deemed to be crucial by advocates of the epigenetic hydrothermal origin of ore-bearing reefs (Jolley et al., 2004). However, the segregation of pyrite as veinlets and zones oriented roughly concordantly to the reef attitude or, less frequently, obliquely or in a fan shape may be explained by petrophysical factors. Differences in gel density; layering of gels; nonuniform and multistage coagulation of colloids; coexistence of a colloidal phase, gel, and true solution; and their displacements may be such factors. The fracture-controlled localization of the late sulfides is expressed not only at the microscopic level, commonly cited as evidence for their epigenetic origin, but also in the development of schistose zones in the Black Reef and oblique zones enriched in pyrrhotite in the VCR. The late sulfide mineralization may be defined as epigenetic with respect to the main pyrite–quartz ore. At the same time, the geochemical data and pyrrhotite and chalcopyrite localization indicate that this mineralization was formed from residual solutions closely related to the general evolution of reefs. The association of the late sulfides with REE mineralization should be mentioned in this respect. Jolley et al. (2004) pointed out an association of pyrrhotite and gold with carbonic matter that contains florencite. Chalcopyrite and pyrrhotite were established in association with allanite and titanite in amygdules located in the hanging wall of the VCR. If this is actually a common mineral assemblage, the time of its formation is determined as definitely after the eruption of the Kliprieversberg Volcanics, the lower unit of the Ventersdorp Supergroup, dated at 2.7 Ga. The timing of hydrothermal mineral assemblages in reefs remains to be specified; however, as follows from the available data, the ore-forming system of the VCR evolved 2.84–2.70 Ga ago. Only uranium mineralization is outside of this interval and had its own geochemical history, which is still to be elucidated on the basis

of the theory of exogenic (epigenetic) deposit formation supported by experience in underground leaching of polyelemental ore (Laverov et al., 1998).

The list of problems that merit further investigation may be continued, although it should be noted that many solutions may be found in the available data and their reconsideration, in particular, taking into account the concept of the primacy of colloidal–disperse systems and complex multifactor relationships in the reef formation. This concept assumes that an enormous source of fluids existed for a long time in the upper mantle and the lower crust beneath the Witwatersrand Basin. The ore-bearing fluids derived from this deep "basin" periodically entered the near-shore zones of this and probably other basins under specific tectonic conditions. The gas state of the fluids explains extensive mass transfer, periodic formation of colloidal–disperse systems, their geochemical similarity, and the unique gold concentration in the basin.

ACKNOWLEDGMENTS

We thank the Anglogold Company (South Africa) and its geological survey and mine geologists for their assistance in collection of samples in 1998, as well as the University of the Witwatersrand (Johannesburg, South Africa) and Professor M. Viljoen and his colleagues for assistance in obtaining data on the Kimberley and Black reefs in 2002. We are grateful to N.S. Bortnikov for his helpful advice and I.V. Murav'eva, B.I. Gongal'sky, T.M. Zlobina, and I.V. Chaplygin for their assistance in preparation of the manuscript. This study was supported by Basic Research Program no. 2 of the Division of Earth Sciences, Russian Academy of Sciences, and by the Russian Foundation for Basic Research (project no. 06-05-64659).

REFERENCES

1. C. R. Anhaeusser and S. Maske, *Mineral Deposits of Southern Africa* (Geol. Soc. South Africa, 1986), Vols. I, II.
2. E. S. A. Antrobus, "The South Rand Goldfield," in *Mineral Deposits of Southern Africa* (Geol. Soc. South Africa, 1986), Vol. I, pp. 689–704.
3. E. S. A. Antrobus, W. C. J. Brink, M. C. Brink, et al., "The Klerksdorp Goldfield," in *Mineral Deposits of Southern Africa* (Geol. Soc. South Africa, 1986), Vol. I, pp. 549–588.
4. F. C. Armstrong, *Genesis of Uranium and Gold-Bearing Precambrian Quartz-Pebble Conglomerates* (US Geol. Surv. Prof. Paper, 1981).
5. E. S. Barton and D. K. Hallbauer, "Trace-Element and U–Pb Isotope Compositions of Pyrite Types in the Proterozoic Black Reef, Transvaal, Sequence, South Africa: Implications on Genesis and Age," Chem. Geol. **133**, 173–199 (1996).
6. A. G. Betekhtin, A. D. Genkin, A. A. Filimonova, and T. N. Shadlun, *Textures and Structures of Ores* (Gosgeoltekhizdat, Moscow, 1958) [in Russian].
7. R. J. Bodnar and M. O. Vityk, "Interpretation of Microterhmometric Data for H_2O–NaCl Fluid Inclusions," in *Fluid Inclusions in Minerals: Methods and Applications* (Siena, Pontignano, 1994), pp. 117–130.
8. A. S. Borisenko, "Cryometric Analysis of the Salt Composition of Gas–Fluid Inclusions in Minerals," Geol. Geofiz. **18** (8), 16–27 (1977).
9. M. B. Borodaevskaya and A. I. Krivtsov, "Role of Colloidal Solutions in Formation of Altered Wall Rocks with Reference to Volcanic-Hosted Massive Sulfide Deposits," in *Problems of Metacomatism* (Nedra, Moscow, 1970), pp. 138–145 [in Russian].
10. P. Brown, "FLINCOR: A Computer Program for the Reduction and Investigation of Fluid Inclusion Data," Am. Mineral. **74**, 1390–1393 (1989).
11. K. D. Card, K. K. Poulsen, and F. Robert, "Archean Superior Province of the Canadian Shield and Its Lode Gold Deposits," Canada Geol. Surv. Paper **19**, 19–33 (1989).
12. F. V. Chukhrov, *Colloids in the Earth's Crust* (Acad. Sci. USSR, Moscow, 1955) [In Russian].
13. M. P. Coward, R. M. Spenger, and C. E. Spenger, "Development of the Witwatersrand Basin, South Africa," in *Early Precambrian Processes* (Geol. Soc. Spec. Publ., 1995), No. 95, pp. 243–269.
14. C. J. Engelbrecht, G. W. S. Baumbach, J. L. Matthysen, and P. Fletcher, "The West Wits Line," in *Mineral Deposits of Southern Africa* (Geol. Soc. South Africa, 1986), Vol. I, pp. 599–648.
15. G. L. England, B. Rasmussen, B. Krapez, and D. I. Groves, "Paleoenvironmental Significance of Rounded Pyrite in Siliciclastic Sequences of the Late Archaen Witwatersrand Basin: Oxygen-Deficient Atmosphere or Hydrothermal Evolution," Sedimentology **49**, 1122–1156 (2002).
16. H. E. Frimmel, D. I. Groves, J. Kirk, et al., "The Formation and Preservation of the Witwatersrand Goldfields, the World's Largest Gold Province," Econ. Geol. **100**, 769–797 (2005).
17. H. E. Frimmel, A. P. Le Roex, J. Knight, and W. E. L. Minter, "A Case Study of Postdepositional Alteration of the Witwatersrand Basal Reef Gold Placer," Econ. Geol. **88**, 249–265 (1993).
18. A. D. Genkin, V. A. Kovalenker, and Yu. G. Safonov, "Ore Textures and Formation Mechanisms of Pipelike Orebodies at the Kochbulak Deposit," in *Methods of Research of Ore-Forming Fluids and Their Assemblages* (Nauka, Moscow, 1980), pp. 127–139 [in Russian].
19. "Geological Studies Related to the Origin and Evolution of the Witwatersrand Basin and Its Mineralization," South African J. Geol. **93** (1), 309 (1990).
20. D. K. Hallbauer, "Geochemistry and Morphology of Mineral Component from the Fossil Gold and Uranium Placers of the Witwatersrand" in *Genesis of Uranium and Gold-Bearing Precambrian Quartz-Pebble Conglomerates* (US Geol. Surv. Prof. Paper, 1981), pp. M1–M22.
21. D. K. Hallbauer, "Geochemistry and Fluid Inclusion in Detrital Minerals As Guides to Their Provenance and Distribution," Geol. Soc. South Africa Spec. Publ., No. 7, 39–57 (1983).
22. D. K. Hallbauer, "The Mineralogy and Geochemistry of Witwatersrand Pyrite, Gold and Uranium, and Carbon-

aceous Matter," in *Mineral Deposits of Southern Africa* (Geol. Soc. South Africa, 1986), Vol. 1, pp. 731–752.

23. D. K. Hallbauer and E. J. D. Kable, "Fluid Inclusions and Trace Element Content of Quartz and Pyrite Pebbles from Witwatersrand Conglomerares: Their Significance with Respect to the Genesis of Primary Deposits," in *Ore Genesis: The State of the Art* (Springer, Berlin, 1982), pp. 742–752.
24. R. W. Hutchinson, "Metallogeny of Precambrian Gold Deposits: Space and Time Relationships," Econ. Geol. **82**, 1993–2007 (1987).
25. R. W. Hutchinson and R. P. Viljoen, "Reevaluation of Gold Source in Witwatersrand Ores," South African J. Geol. **91** (2), 157–173 (1988).
26. S. J. Jolley, S. R. Freeman, A. C. Barnicoat, et al., "Structural Controls on Witwatersrand Gold Mineralization," J. Structural Geology **26**, 1067–1086 (2004).
27. Yu. P. Kazansky, A. F. Belousov, V. G. Petrov, et al., *Sedimentary Rocks (Classification, Characteristics, Genesis)* (Nauka, Novosibirsk, 1987) [in Russian].
28. I. N. Kigai, "Role of Colloids in Hydrothermal Ore Formation," in *Problems of Endogenic Ore Formation* (Nauka, Moscow, 1974), pp. 32–67 [in Russian].
29. J. Kirk, J. Chesley, S. Titley, and J. Walshe, "A Detrital Model for the Origin of Gold and Sulfides in the Witwatersrand Basin Based on Re–Os Isotopes," Geochim. Cosmochim. Acta **65**, 2149–2159 (2001).
30. M. M. Konstantinov, *Noble Metal Provinces* (Nedra, Moscow, 1991) [in Russian].
31. A. A. Kremenetsky and I. Iordan, "Volcanic Sedimentary Genesis of Gold-Bearing Conglomerates in the Witwatersrand (South Africa)," in *Metamorphism of Volcanic Sedimentary Deposits* (Karelian Sci. Center, Russian Acad. Sci., Petrozavodsk, 1996), pp. 63–66 [in Russian].
32. A. A. Kremenetsky and N. A. Yushko, "Role of Sedex-Process in the Formation of Large Economic Gold Resources in Precambrian Paleobasins," in *Proceeding of Sci. Conference on Models of Volcanic-Sedimentary Ore-Forming Systems* (VSEGEI, St. Petersburg, 1999), pp. 100–103.
33. A. A. Kremenetsky, N. A. Yushko, and I. Ye. Maksimyuk, "Hydrothermal Formation of Precambrian Auriferous Conglomerates," in *Mineral Deposits Research and Exploration: Where Do They Meet?* (Balkema, Rotterdam, 1997), pp. 221–224.
34. A. A. Kremenetsky, N. A. Yushko, and I. E. Maksimyuk, "Typomorphic and Typochemical Features of Quartz and Pyrite As Criteria for the Sedex Genesis of the Witwatersrand Deposits (South Africa)," in *Proceedings of Sci. Conference on Applied Mineralogy for Forecasting, Exploration and Appraisal of Mineral Deposits* (Moscow, 2001), p. 24.
35. F. P. Krendelev, *Metalliferous Conglomerates of the World* (Nauka, Novosibirsk, 1974) [in Russian].
36. S. G. Kryazhev, Yu. V. Vasyuta, and M. K. Kharrasov, "Technique of Bulk Analysis of Inclusions in Quartz," in *Proceedings of XI Intern. Conference on Thermobarogeochemistry* (VNIISIMS, Aleksandrov, 2003), pp. 6–10.
37. N. P. Laverov, "Uranium Deposits, Their Geochronology and General Distribution Patterns," in *Principles of the Forecasting of Uranium Ore Provinces and Districts* (Nedra, Moscow, 1986) [in Russian].
38. J. D. M. Law and G. N. Phillips, "Hydrothermal Replacement Model for Witwatersrand Gold," Econ. Geol. **100**, 799–811 (2005).
39. N. P. Laverov, I. G. Abdul'manov, K. G. Brovin, et al., *Underground Leaching of Multicomponent Ores* (Acad. Mining Sci., Moscow, 1998) [in Russian].
40. N. P. Laverov, V. V. Distler, G. L. Mitrofanov, et al., "Platinum and Other Native Metals in Ores of the Sukhoi Log Gold Deposit," Dokl. Akad. Nauk **355** (5), 664–668 (1997) [Dokl. Earth Sci. **355A** (6), 904–907 (1997)].
41. J. D. M. Law, A. C. Bailey, A. B. Cadle, et al., "Reconstructive Approach to the Classification of Witwatersrand 'Quartzites'," South African J. Geol. **93** (1), 83–92 (1990).
42. L. M. Lebedev, *Metacolloides in Endogenic Deposits* (Nauka, Moscow, 1965) [in Russian].
43. I. E. Maksimyuk and A. A. Kremenetsky, "Composition and Origin of Organic Matter in Witwatersrand Conglomerates: New Data," in *Proceedings of Sci. Conference on Traditional and New Lines in Mineralogical Studies* (IGEM–VIMS, Moscow, 2001), pp. 90–92.
44. W. E. L. Minter, "Detrital Gold, Uranium and Pyrite Concentration Related to Sedimentology in Precambrian Vaal Reef Placer, Witwatersrand, South Africa," Econ. Geol. **71**, 157–176 (1976).
45. W. E. L. Minter and J. S. Loen, "Paleocurrent Dispersal Patterns of Witwatersrand Gold Placers," South African J. Geol. **94**, 70–85 (1991).
46. W. E. L. Minter, W. C. N. Hill, R. J. Kidger, et al., "The Welcom Goldfield," in *Mineral Deposits of Southern Africa* (Geol. Soc. South Africa, 1986), Vol. 1, pp. 497–540.
47. R. E. Myers, T. S. McCarthy, and I. G. Stanistreet, "A Tectono-Sedimentary Reconstruction of the Development and Evolution of the Witwatersrand Basin, with Particular Emphasis on the Central Rand Group," South African J. Geol. **93** (1), 180–201 (1990).
48. G. N. Phillips, "Metamorphism of the Witwatersrand Goldfields: Conditions during Peak Metamorphism," J. Metamorph. Geol. **5**, 307–322 (1987).
49. G. N. Phillips and R. E. Myers, "The Witwatersrand Gold Fields: Part II. Postdepositional History, Synsedimentary Processes and Gold Distribution," Econ. Geol. **84**, 598–608 (1989).
50. G.N. Phillips, J. D. M. Law and G. Stevens, "Alteration, Heat and Witwatersrand Gold: 111 Years after Harrison and Langlaagte," South African J. Geol. **100**, 377–392 (1997).
51. G. N. Phillips, R. E. Myers, J. D. M. Law, et al., "The Witwatersrand Gold Fields: Part I. Postdepositional History, Synsedimentary Processes and Gold Distribution," Econ. Geol. **84**, 585–597 (1989).
52. V. V. Popov, N. I. Stuchevsky, and Yu. I. Demin, *Base-Metal Deposits of the Rudny Altai* (IGEM, Moscow, 1995) [in Russian].
53. A. M. Portnov, "On Possible Hypogene Origin of the Witwatersrand Conglomerates," Izv. Vyssh. Uchebn. Zaved., Geol. Razved., No. 10, 49–58 (1988).
54. V. Yu. Prokof'ev, "Types of Hydrothermal Ore-Forming Systems As Deduced from Fluid Inclusion Studies," Geol. Rudn. Mestorozhd. **40** (6), 514–528 (1998) [Geol. Ore Deposits **40** (6), 457–470 (1998)].

55. P. Ramdohr, "New Observations on the Ores of the Witwatersrand in South Africa and Their Genetic Significance," Trans. Geol. Soc. South Africa **6**, 1–50 (1958).

56. D. V. Rundquist, "Epochs of Rejuvenation of the Precambrian Crust and Their Metallogenic Implications," Geol. Rudn. Mestorozhd. **35** (6), pp. 467–480 (1993).

57. D. V. Rundquist, "Factor of Time in the Formation of Hydrothermal Deposits: Periods, Epochs, Megastages, and Stages of Ore Formation," Geol. Rudn. Mestorozhd. **39** (1), 11–24 (1997) [Geol. Ore Deposits **39** (1), 8–19 (1997)].

58. R. Saager, "Geochemical Studies of the Origin of the Detrital Pyrites in the Conglomerates of the Witwatersrand Goldfields, South Africa," in *Genesis of Uranium and Gold-Bearing Precambrian Quartz-Pebble Conglomerates* (US Geol. Surv. Prof. Paper, 1981), pp. L1–L17.

59. R. Saager, T. Utter, and M. Meyer, "Pre-Witwatersrand and Witwatersrand Conglomerates in South Africa: A Mineralogical Comparison and Bearings of the Genesis of Gold–Uranium Placers," in *Ore Genesis: The State of the Art* (Springer, Berlin, 1982), pp. 38–56.

60. Yu. G. Safonov, "Hydrothermal Gold Deposits: Abundance, Geological and Genetic Types, and Productivity of Ore-Forming Systems," Geol. Rudn. Mestorozhd. **39** (1), 25–40 (1997) [Geol. Ore Deposits **39** (1), 20–32 (1997)].

61. Yu. G. Safonov, "Gold and Gold-Bearing Deposits of the World: Genesis and Metallogenic Potential," Geol. Rudn. Mestorozhd. **45** (4), 305–320 (2003) [Geol. Ore Deposits **45** (4), 265–278 (2003)].

62. Yu. G. Safonov, "Formation of Gold Deposits," in *Problems of Ore Geology, Petrology, Mineralogy, and Geochemistry* (IGEM RAS, Moscow, 2004a), pp. 99–129 [in Russian].

63. Yu. G. Safonov, "Role of Gaseous Fluids and Colloidal Solutions in Formation of Gold-Bearing Reefs of Witwatersrand," in *Proceedings of the 32nd Session of IGC* (Florence, 2004b), Vol. 2.

64. Yu. G. Safonov, L. V. Bershov, B. A. Bogatyrev, et al., "Gold–Uranium Ores of the Witwatersrand (South Africa): Evidence for Sedimentary and Hydrothermal Genesis," in *Proceedings of the 1st All-Russia Lithological Conference* (Moscow, 2000), Vol. 2, pp. 194–199.

65. Yu. G. Safonov, L. V. Bershov, B. A. Bogatyrev, and A. G. Bushev, "Organic Matter in Ores of the Witwatersrand Deposit," in *Proceedings of Sci. Conference on Traditional and New Lines in Mineralogical Studies* (IGEM–VIMS, Moscow, 2001), pp. 135–137.

66. Yu. G. Safonov and N. M. Kassim, "Gold–Pyrite Mineral Assemblage of the Gold-Bearing Reefs of Witwatersrand," in *Proceedings of the 11 Quadrennial IAGOD Symposium and Geocongress, Late Abstracts* (Windhoek, 2002), pp. 15–18.

67. M. Schidlovski, "Uraniferous Constituents of the Witwatersrand Conglomerates: Ore-Microscopic Observations and Implications for the Witwatersrand Metallogeny," in *Genesis of Uranium and Gold-Bearing Precambrian Quartz-Pebble Conglomerates* (US Geol. Surv. Prof. Paper, 1981), pp. N1–N29.

68. A. D. Shcheglov, *On the Metallogeny of the Republic of South Africa, Genesis of the Witwatersrand Gold Deposits, and Outlooks for Discovery of Their Analogues in Russia* (VSEGEI, St. Petersburg, 1994).

69. N. A. Shilo, *Theory of Placers* (Dal'nauka, Vladivostok, 2002) [in Russian].

70. N. A. Shilo and M. S. Sakharova, "Origin of Pyrites from Witwatersrand Deposits," Geol. Rudn. Mestorozhd. **30** (2), 85–89 (1988).

71. D. I. Tsarev, "Metalliferous Pseudoconglomerates of the Witwatersrand," in *Precambrian Metallogeny and Metamorphic Ore Formation* (Kiev, 1990), Part 2, pp. 184–186 [in Russian].

72. D. I. Tsarev, *Metasomatism* (Buryat. Sci. Center, Siberian Division, Russ. Acad. Sci., Ulan-Ude, 2002) [in Russian].

73. R. E. Tucker and R. P. Viljoen, "The Geology of the West Rand Goldfield, with Special Reference of the Southern Limb," in *Mineral Deposits of Southern Africa* (Geol. Soc. South Africa, 1986), Vol. 1, pp. 649–688.

74. E. B. Tweedie, "The Evander Goldfield," in *Mineral Deposits of Southern Africa* (Geol. Soc. South Africa, 1986), Vol. 1, pp. 705–730.

75. D. T. Vermaakt and I. E. Chunett, "Tectono-Sedimentary Processes which Controlled the Deposition of the Ventersdorp Contact Reef within the West Wits Line," in *Proceedings of XV CMMI Congress* (Johannesburg, 1994), Vol. 3, pp. 117–130.

76. R. P. Viljoen, R. Saager, and M. J. Viljoen, "Some Thoughts on the Origin and Processes Responsible for the Concentration Gold in the Early Precambrian of Southern Africa," Miner. Deposita **5**, 164–180 (1970).

77. A. Vollbrecht, T. Oberthur, J. Ruedrich, and K. Weber, "Microfabric Analyses Applied to the Witwatersrand Gold and Uranium-Bearing Conglomerates: Constraints on the Provenance and Post-Depositional Modification of Rock and Ore Components," Miner. Deposita **37**, pp. 433–451 (2002).

78. H. C. M. Whiteside, "Examples of Movement of Gold in Solution in the Witwatersrand: Ventersdorp and Transvaal Systems," in *Genesis of Uranium- and Gold-Bearing Precambrian Quartz-Pebble Conglomerates* (US Geol. Surv. Prof. Paper, 1981), pp. I1–I4.

79. R. Woodall, "Gold in Australia," in *Economic Geology of Australia and Papua New Guinea* (Melbourne, 1990), pp. 45–68.

80. O. V. Yapaskurt, *Principles of Lithogenesis* (Moscow State Univ., Moscow, 2005) [in Russian].